OSPAR COMMISSION

Assessment of Atmospheric Lead, Cadmium and Mercury Pollution to the OSPAR Maritime Area in 2020

Hazardous Substances and Eutrophication Series

2023

OSPAR Convention

The Convention for the Protection of the Marine Environment of the North-East Atlantic (the “OSPAR Convention”) was opened for signature at the Ministerial Meeting of the former Oslo and Paris Commissions in Paris on 22 September 1992. The Convention entered into force on 25 March 1998. The Contracting Parties are Belgium, Denmark, the European Union, Finland, France, Germany, Iceland, Ireland, Luxembourg, the Netherlands, Norway, Portugal, Spain, Sweden, Switzerland and the United Kingdom.

Convention OSPAR

La Convention pour la protection du milieu marin de l'Atlantique du Nord-Est, dite Convention OSPAR, a été ouverte à la signature à la réunion ministérielle des anciennes Commissions d'Oslo et de Paris, à Paris le 22 septembre 1992. La Convention est entrée en vigueur le 25 mars 1998. Les Parties contractantes sont l'Allemagne, la Belgique, le Danemark, l’Espagne, la Finlande, la France, l’Irlande, l’Islande, le Luxembourg, la Norvège, les Pays-Bas, le Portugal, le Royaume-Uni de Grande Bretagne et d’Irlande du Nord, la Suède, la Suisse et l’Union européenne.

MSC-E

Meteorological Synthesizing Centre - East (MCS-E)

2nd Roshchinsky proezd, 8/4, 115419 Moscow, Russia
Phone.: +7 926 292 00 18
E-mail: msce@msceast.org
Internet: www.msceast.org

OSPAR Commission

The Aspect, 12 Finsbury Square
London EC2A 1AS United Kingdom
Telephone: +44 (0) 20 7430 5200
Email: secretariat@ospar.org

Assessment of Atmospheric Lead, Cadmium and Mercury Pollution to the OSPAR Maritime Area in 2020

Ilia Ilyin, Oleg Travnikov, Olga Rozovskaya

ACKNOWLEDGEMENTS

Model assessment of atmospheric input of Pb, Cd and Hg to the OSPAR maritime area was jointly funded by OSPAR Commission and Cooperative Programme for Monitoring and Evaluation of the Long-range Transmission of Air Pollutants in Europe (EMEP). MSC-E is grateful to colleagues from CEIP and CCC of EMEP for providing us with emission and measurement data. The authors also wish to thank Irina Strizhkina for preparation of the graphics and other editorial work.

EXECUTIVE SUMMARY

Model assessment of atmospheric pollution of the OSPAR maritime area by heavy metals in 2020 was carried out. The assessment includes the information on time series of lead (Pb), cadmium (Cd) and mercury (Hg) emissions in the OSPAR Contracting Parties for the period from 1990 to 2020, sectoral emissions in these countries in 2020, deposition of Pb, Cd and Hg to the OSPAR regions in 2020 and their trends for the period 1990-2020. Besides, evaluation of the modelling results against measurement data is presented.

Total Pb, Cd and Hg emission in the OSPAR Contracting Parties as a whole in 2020 amounted to 483, 32 and 20 tonnes, respectively. Reduction of Pb, Cd and Hg atmospheric emissions in the OSPAR Contracting Parties from 1990 to 2020 was 97%, 76% and 86%, respectively. The largest reduction of Pb is noted for France and Sweden (98% each). Finland is known for the most significant (90%) decrease of Cd emission. The strongest reduction of Hg emission was reached in Denmark (93%). Emissions of Pb, Cd and Hg are characterized by stronger reduction rate in the first decade of the considered period compared to the reduction from 2000 to 2020.

Reported heavy metal emission data for the OSPAR Contracting Parties are split into 13 emission source categories (sectors). Contributions of emission sectors to total emission were analysed. The main emission sectors contributing to the OSPAR Pb emission are B_Industry (45%), F_RoadTransport (32%) and C_OtherStatComb (10%). The main contribution to Cd total emission is made by the sector B_Industry (58%), followed by C_OtherStatComb (14%) and E_Solvents (11%). The sectors B_Industry (46%) and A_PublicPower (29%) are the largest contributors to total Hg emissions in the OSPAR countries.

The highest spatial mean deposition fluxes of Pb (0.29 kg/km^2/y) and Cd (10.3 g/km^2/y) in 2020 were noted for Region II. The lowest fluxes (0.14 kg/km^2/y and 5.1 g/km^2/y, respectively) took place in Region I. In case of Hg, Region I is characterized by the highest (8.9 g/km^2/y), and Region IV - by the lowest (4.8 g/km^2/y) spatial mean deposition flux. Deposition of Pb, Cd and Hg to the OSPAR maritime area substantially declined from 1990 to 2020. The strongest decline of Pb, Cd and Hg deposition took place in Region II (Greater North Sea) and amounted to 87%, 81% and almost 50%, respectively. The decline of deposition to the OSPAR regions is smaller than the emission reduction because of the effect of secondary and global sources.

Evaluation of the modelling results against measurements demonstrated that the model tends to somewhat overestimate observed concentrations of Pb and Cd in air. The agreement between modelled and observed Hg concentrations in air is within ±15% at most of stations. Wet deposition of Pb, Cd and Hg were reproduced with mean relative bias of -26%, -42% and 16%, respectively. For the majority of stations the modelled and observed concentrations and deposition fluxes agree within a factor of two.

RÉCAPITULATIF

Un modèle d'évaluation de la pollution atmosphérique de la zone maritime OSPAR par les métaux lourds en 2020 a été réalisé. L'évaluation comprend des informations sur les séries temporelles des émissions de plomb (Pb), de cadmium (Cd) et de mercure (Hg) dans les Parties contractantes OSPAR pour la période allant de 1990 à 2020, les émissions sectorielles dans ces pays en 2020, les dépôts de Pb, Cd et Hg dans les Régions OSPAR en 2020 et leurs tendances pour la période 1990-2020. En outre, l'évaluation des résultats de la modélisation par rapport aux données de mesure est présentée.

Les émissions totales de Pb, Cd et Hg dans l'ensemble des Parties contractantes OSPAR en 2020 s'élevaient à 483, 32 et 20 tonnes, respectivement. La réduction des émissions atmosphériques de Pb, Cd et Hg dans les Parties contractantes OSPAR de 1990 à 2020 était de 97%, 76% et 86%, respectivement. La réduction la plus importante de Pb est observée en France et en Suède (98% chacun). La Finlande est connue pour la réduction la plus importante (90%) des émissions de Cd. La plus forte réduction des émissions de Hg a été atteinte au Danemark (93%). Les émissions de Pb, Cd et Hg se caractérisent par un taux de réduction plus important au cours de la première décennie de la période considérée par rapport à la réduction entre 2000 et 2020.

Les données d'émission de métaux lourds rapportées pour les parties contractantes OSPAR sont réparties en 13 catégories de sources d'émission (secteurs). Les contributions des secteurs d'émission aux émissions totales ont été analysées. Les principaux secteurs d'émission contribuant aux émissions de Pb d'OSPAR sont B_Industrie (45%), F_Transport routier (32%) et C_AutresStatComb (10%). La principale contribution aux émissions totales de Cd est apportée par le secteur B_Industrie (58%), suivi par C_AutresStatComb (14%) et E_Solvants (11%). Les secteurs B_Industrie (46%) et A_PublicPower (29%) sont ceux qui contribuent le plus aux émissions totales de Hg dans les pays OSPAR.

Les flux de dépôts moyens spatiaux de Pb (0,29 kg/km2/an) et de Cd (10,3 g/km^2/an) les plus élevés en 2020 ont été observés dans la Région II. Les flux les plus faibles (0,14 kg/km^2/an et 5,1 g/km^2/an, respectivement) ont eu lieu dans la Région I. Dans le cas du Hg, la région I se caractérise par le flux de dépôt spatial moyen le plus élevé (8,9 g/km^2/an), et la région IV par le flux de dépôt spatial moyen le plus faible (4,8 g/km^2/an). Les dépôts de Pb, Cd et Hg dans la zone maritime OSPAR ont considérablement diminué entre 1990 et 2020. La plus forte diminution des retombées de Pb, Cd et Hg a eu lieu dans la Région II (mer du Nord au sens large) et s'est élevée à 87 %, 81 % et presque 50 %, respectivement. La diminution des retombées dans les Régions OSPAR est inférieure à la réduction des émissions en raison de l'effet des sources secondaires et mondiales.

L'évaluation des résultats de la modélisation par rapport aux mesures a montré que le modèle tend à surestimer quelque peu les concentrations observées de Pb et de Cd dans l'air. La concordance entre les concentrations modélisées et observées de Hg dans l'air est de ±15 % dans la plupart des stations. Les dépôts humides de Pb, Cd et Hg ont été reproduits avec un biais relatif moyen de -26 %, -42 % et 16 %, respectivement. Pour la majorité des stations, les concentrations et les flux de dépôt modélisés et observés concordent avec un facteur de deux.

CONTENTS

1. INTRODUCTION

Heavy metals and their compounds are known for their toxicity and harmful effects on human health and biota. They are multi-organ toxicants and adversely affect neurological, cardiovascular, renal, gastrointestinal, hematological and reproductive systems of humans [*Mitra et al*., 2022; *ECHA*, 2013; *ECHA*, 2018; *Rice et al*., 2014; *Karcioglu and Arslan*, 2019]. In the environment, heavy metals are toxic to plants, animals and micro-organisms [*Naeem et al*., 2020]. In particular, they can bioaccumulate in food webs and cause harm to marine life [*Gheorghe et al.,* 2017; *Jin et al.,* 2021; *Shah,* 2021]. Heavy metals enter the marine environment through various routes including direct discharges, riverine inputs and atmospheric deposition. In spite of the progress in reduction of atmospheric emissions reached due to Aarhus Protocol on Heavy Metals of the UN ECE Convention on Long-Range Transboundary Air Pollution [*UNECE*, 2012], the atmospheric pathway remains an important contributor to the marine environment providing from one fifth to two thirds of the total heavy metal input [*OSPAR*, 2017].

This report is focused on the assessment of atmospheric loads of lead (Pb), cadmium (Cd) and mercury (Hg) to the maritime area of Convention for the Protection of the Marine Environment of the North-East Atlantic (OSPAR) in 2020. The assessment was carried out by Meteorological Synthesizing Centre-East of the Co-operative Programme for Monitoring and Evaluation of the Long Range Transmission of Air Pollutants in Europe (EMEP) at the request of the OSPAR Commission. The assessment includes analysis of emission data in the OSPAR Contracting Parties and atmospheric deposition of Pb, Cd and Hg to the OSPAR maritime area in 2020 and their long-term changes from 1990 to 2020. Current work continues the previous assessment of heavy metal pollution of the OSPAR waters [*Ilyin et al*., 2022].

The data products were prepared in accordance with the *Contract for EMEP/MSC-E products on emissions and atmospheric deposition of heavy metals in support of NEAES Strategic Objectives 1 and 2 to achieve clean seas in the OSPAR marine area* and consist of the following deliverables:

1. Update of time series of total annual emissions (1990-2019) of Pb, Cd and Hg from OSPAR Contracting Parties with data for 2020 including contribution of emission sectors (based on official EMEP reporting 2022).
2. Update of time series of total annual atmospheric deposition of Pb, Cd and Hg to the OSPAR areas with modelling data for 2020 (based on regular EMEP modelling for the OSPAR regions II, III, and IV and additional global simulations for the OSPAR regions I and V).
3. Technical note and data tables summarizing information on emissions and deposition data.

Emission data, including long-term time series and sectoral composition in 2020 in the OSPAR Contracting Parties are presented in Chapter 3. Chapter 4 is focused on atmospheric deposition of Pb, Cd and Hg in 2020 to the OSPAR maritime area and long-term trends of deposition fluxes. In addition to this, modelled concentrations and deposition fluxes were compared with the available monitoring data. The results of the model evaluation are summarized in Chapter 5. Main outcomes of the work are overviewed in the Conclusions section. Tables with data products and results of the model evaluation against measurements are compiled in Annexes A and B, respectively.

2. Assessment approach

Assessment of Pb, Cd and Hg pollution levels was carried out using the Global EMEP Multi-media Modelling System (GLEMOS), version v2.2.2. The model simulations were performed on both regional (EMEP domain, https://www.ceip.at/the-emep-grid) and global scales. Anthropogenic emission data for modelling of the pollutants for the period 1990-2020 were prepared based on the EMEP emissions reporting (Chapter 3).

Data on wind re-suspension of particle-bound heavy metals (Pb and Cd) from soil and seawater were generated using the dust pre-processor [*Gusev et al*., 2006; 2007]. Data on background topsoil concentrations of heavy metals is derived from the results of the FOREGS programme [*Salminen,* 2005]. In order to take into account long-term accumulation over a long-term period, spatially distributed enrichment factors for concentrations in soils were utilized. It is assumed that the enrichment factor is proportional to the accumulated deposition. The enrichment of sea-salt aerosol with Pb and Cd was calculated based on [*Richardson et al.*, 2001].

Prescribed fluxes of natural and secondary Hg^0 re-emissions from soil and seawater were generated depending on Hg concentration in soil, soil temperature, and solar radiation for emissions from land and proportional to the primary production of organic carbon in seawater for emissions from the ocean [*Travnikov and Ilyin*, 2009]. Additionally, prompt re-emission of Hg from snow is taken into account using an empirical parametrization based on the observational data [*Kirk et al.,* 2006; *Johnson et al.,* 2008; *Ferrari et al*., 2008].

Meteorological data for 2020 are based on operational analysis data of European Centre for Medium Range Weather Forecasts (ECMWF). Original meteorological data were processed by meteorological pre-processor based on the Weather Research and Forecast modelling system (WRF) [*Skamarock et al.*, 2008]. Atmospheric concentrations of chemical reactants (O_3, OH^-, SO_2, NO_3^- and Br^-), which are required for description of Hg chemistry, were derived from the MOZART and p-TOMCAT models [*Emmons et al.,* 2010; *Yang et al.,* 2005; 2010].

Boundary conditions for the regional scale simulations of all considered pollutants were obtained from the GLEMOS model runs on a global scale. Initial conditions were generated with one-month spin-up model runs for regional simulations and a three-year spin-up run for the global-scale Hg modelling.

Assessment of pollution levels is carried out for five regions of the OSPAR maritime area: Region I – Arctic Waters; Region II – Greater North Sea; Region III – the Celtic Seas; Region IV – Bay of Biscay and Iberian Coast, and Region V – Wider Atlantic (Fig. 1). Regions II, III and IV are fully covered by the EMEP modelling domain, while parts of Regions I and V lie outside the EMEP borders. In order to prepare data on deposition to the entire areas of Regions I and V global-scale modelling was carried out. The merging procedure for the global and regional modelling results is described in [*Ilyin et al*., 2022].

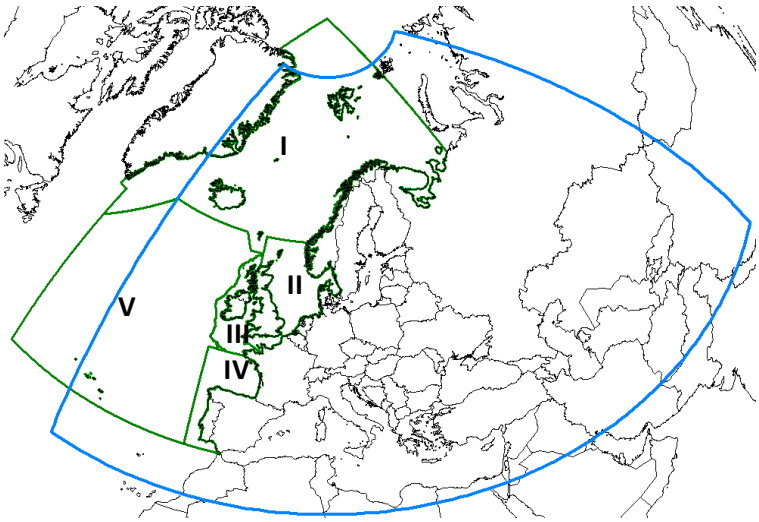

Fig. 1. *Border of the EMEP domain (blue line) and OSPAR maritime area (green line) with indication of the OSPAR regions (I – V).*

To characterize long-term changes of heavy metal pollution levels the bi-exponential approximation of trends was applied [*Colette et al.*, 2016]. The changes of heavy metal pollution levels in the period from 1990 to 2020 are typically non-linear with faster decline in nineties and slower change thereafter. The bi-exponential approach assumes that long-term changes are approximated by "fast" exponent well describing the reduction in the beginning of the period, and "slow" exponent explaining the decline after the nineties (1):

$$C(t) = a_1 \cdot \exp\left(-\frac{t}{\tau_1}\right) + a_2 \cdot \exp\left(-\frac{t}{\tau_2}\right) \quad (1)$$

Here $C(t)$ is approximated deposition or concentration at time t; τ_1 and τ_2 are characteristic times; and a_1 and a_2 are coefficients.

Long-term changes of deposition are characterized by total change for the whole period (2) and mean relative annual rate of change (3):

$$R_{tot} = \frac{(C_{beg} - C_{end})}{C_{beg}} = 1 - \frac{C_{end}}{C_{beg}} \quad (2)$$

$$R_{av} = 1 - \left(\frac{C_{end}}{C_{beg}}\right)^{\frac{1}{N-1}} \quad (3)$$

Average rate of change is geometric mean of the annual changes between two neighbouring years. C_{beg} and C_{end} are the trend values of the first and the final years of the considered period and N is number of considered years.

Significance of the calculated long-term trends was evaluated using nonparametric Mann-Kendall test [*Gilbert*, 1987]. This test is widely used in air pollution research and, in particular, in assessment

of long-term trends of atmospheric pollutants in the EMEP countries [*Colette et al.,* 2016]. Unlike typically used statistical methods, the Mann-Kendall's approach does not require assumption of any statistical (e.g., normal) distribution of the analyzed data. In this work the significance of trends was tested at significance levels of 0.05, 0.01 and 0.001.

Statistical indicators used for comparison of modelled and observed values include mean relative bias (MRB) and Pearson's coefficient of correlation (R_c), calculated by formulas (4) and (5), respectively:

$$MRB = \frac{(\bar{M} - \bar{O})}{\bar{O}} \cdot 100\% \quad (4)$$

$$R_c = \frac{\sum_1^N (M - \bar{M}) \cdot (O - \bar{O})}{\sqrt{\sum_1^N (M - \bar{M})^2 \cdot \sum_1^N (O - \bar{O})^2}} \quad (5)$$

In (4) and (5) modelled values are denoted as M and observed values as O. Besides, a fraction of stations, where discrepancy between modelled and observed values lies within a factor of 2 (F2), was determined.

Prior to the comparison, the outliers in raw measurement data were identified and filtered out. In order to identify the outliers in time series of each year the standard deviation method was applied [e.g., *Bain and Engelhardt*, 1992]. The method defines the outlier as a value falling outside the range of <M>±(3*SD), where <M> is the mean value, and SD is the standard deviation. This method was applied for concentrations in air and in precipitation. Due to gaps caused by missing or incorrect measurements or filtering out of outliers the time series of each year are often incomplete. Annual mean measured concentrations or annual sums of wet deposition were not used in the analysis if their completeness was below 50%.

3. Emissions of Pb, Cd and Hg in the OSPAR Contracting Parties

Emission data covering the period from 1990 to 2020 used in the model assessment are prepared by the EMEP Centre on Emission Inventories and Projections (CEIP) (http://www.ceip.at/). For most of the EMEP countries total emissions of Pb, Cd and Hg officially reported to the UN ECE Secretariat are used. For countries, which do not submit their emission data, expert estimates of emissions are elaborated based on of methodology developed by CEIP [*Tista et al.,* 2019]. For the consistency purposes emission data for the period from 1990 to 2019 used in current study are the same as those used in previous assessment [*Ilyin et al*., 2022]. Emissions for 2020 are based on the EMEP reporting of emissions data in 2022.

In order to simulate deposition fluxes over the entire area of the Regions I and V global-scale model calculations of Pb, Cd and Hg transport were performed. Besides, the results of global-scale calculations are necessary for generation of boundary concentrations used in the model calculations over the EMEP grid. Global gridded emissions of Pb, Cd and Hg were prepared by MSC-E [*Ilyin et al.,* 2022].

Along with gridded emission data additional emission parameters are required. They include seasonal variations, vertical distribution and chemical speciation of emissions. Required vertical and temporal disaggregation of the emissions was generated using emission pre-processing tool, developed by MSC-E for the GLEMOS modelling system. More detailed information on the emission pre-processing procedure is presented in the heavy metal Status Report [*Ilyin et al.,* 2018].

Sectoral emission data in the OSPAR Contracting Parties are prepared for the following gridded NFR (Nomenclature For Reporting) emission sectors (A_PublicPower; B_Industry; C_OtherStatComb; D_Fugitive; E_Solvents; F_RoadTransport; G_Shipping; H_Aviation; I_Offroad; J_Waste; L_AgriOther and M_Other) used in the model assessments within the EMEP programme. Emission of each gridded NFR (GNFR) sector is a result of aggregation of particular NFR sectors. Detailed description of GNFR sectors is available in EMEP/EEA Air Pollutant Emission Inventory Guidebook [*Guidebook*, 2019] and in Table A.2.

Total Pb, Cd and Hg emission in the OSPAR Contracting Parties as a whole in 2020 amounted to 483, 32 and 20 tonnes, respectively (Tables A.3 – A.5). The highest emission values of these metals in 2020 were noted for Germany. German emissions of Pb, Cd and Hg in 2020 made up 143, 11, and 6 tonnes, respectively. Other major OSPAR countries-emitters were the United Kingdom, Spain and France. Contribution of these four countries to total OSPAR emission was 80% for Pb and 74% for Cd and Hg. The lowest heavy metal emissions took place in Iceland and Luxembourg.

Time series of Pb, Cd and Hg total annual emissions in the OSPAR Contracting Parties in 1990 – 2020 are shown in Fig. 2-4. Emission of Pb in the OSPAR countries reduced by 97%. The highest reduction took place in France and Sweden (98% each). Besides, in Ireland, Norway, the United Kingdom and Spain the reduction was higher (97 – 98%) than the average value for the OSPAR countries. In Iceland Pb emission demonstrated an increase until 2007 and then general decline that finally resulted to

about 80% increase relative to 1990. Reduction of total Cd emissions in the OSPAR countries made up 76%, ranging from 3% in the Netherlands to 90% in Finland. Large reduction (82% – 88%) was also noted for France, Switzerland, Belgium, Sweden and the United Kingdom. Emissions of Hg decreased from 1990 to 2020 by 86% in the OSPAR countries. The highest reduction was reached in Denmark (93%), followed by the United Kingdom (91%), France (91%) and Switzerland (90%). Besides, in Iceland, the Netherlands and Norway the reduction was also higher (86%–89%) than the average for the OSPAR countries as a whole. Portugal is characterized by the lowest Hg reduction (45%) among the OSPAR Contracting Parties. Emissions of Pb, Cd and Hg were characterized by stronger rate of reduction in the first decade of the considered period compared to the reduction from 2000 to 2020. In terms of absolute values, the most significant reduction of emissions from 1990 to 2020 was reported for Germany, France, the United Kingdom and Spain. In particular, the highest reduction of Pb emissions took place in France (about 4220 tonnes), of Cd – in Spain (22 tonnes) and of Hg – in the United Kingdom (around 35 tonnes).

Most of the OSPAR contracting Parties demonstrated relatively gradual long-term decline of national emissions of Pb, Cd and Hg. However, in some cases marked inter-annual variability of national totals took place. For example, annual totals of Cd emissions in the Netherlands in the 1990 – 2020 period were represented by a sequence of peaks and dips. Analysis of emission sectors revealed that these sharp changes in emissions were mainly conditioned by the GNFR sector B_Industry, or, in particular, by NFR sectors 1A2C (Stationary combustion in manufacturing industries and construction: Chemicals), 2B10a (Chemical industry: Other), 2C1 (Iron and steel production) and 2C6 (Zinc production) (Fig. A.1a) [*CEIP*, 2022]. The changes in estimates of Cd emissions between 2017 and 2018 are explained by changes in emission measurement methodology [*Wever et al.,* 2020].

Another example of non-typical emission time series is emissions of Cd and Pb in Iceland. The emissions had been rising since 1993 to 2007 and then declined until 2020. The main contributor to the emissions was sector A_PublicPower (Fig. A.1b). In 1993 waste incineration with energy recovery started. Emission from this activity was attributed to the A_PublicPower sector. Amount of energy produced by waste incineration peaked in 2007, and since then this amount had been declining until 2013. After 2013 this activity was stopped [*Keller et al*., 2020]. Besides, significant contributor to Pb emissions was the use of fireworks attributed to the sector E_Solvents. Growing contribution of emissions from the use of firework reached its peak in 2007, and then tended to grow down because of economic decline.

The main emission sectors contributing to Pb emissions in the OSPAR countries were B_Industry (45%), F_RoadTransport (32%) and C_OtherStatComb (10%) (Table A.6). The main activities contributing around 70% to GNFR sector B_Industry included production of glass, iron and steel, and stationary combustion in manufacturing industries and construction (Table A.9). The main contributor to the Road Transport sector was automobile tyre and brake wear, followed by emissions from passenger cars. These two activities made up 95% of total emission of the Road Transport sector. NFR sectors ‘Commercial/Institutional: Stationary’ and ‘Residential: Stationary’ added up 94% to emissions in GNFR sector C_OtherStatComb.

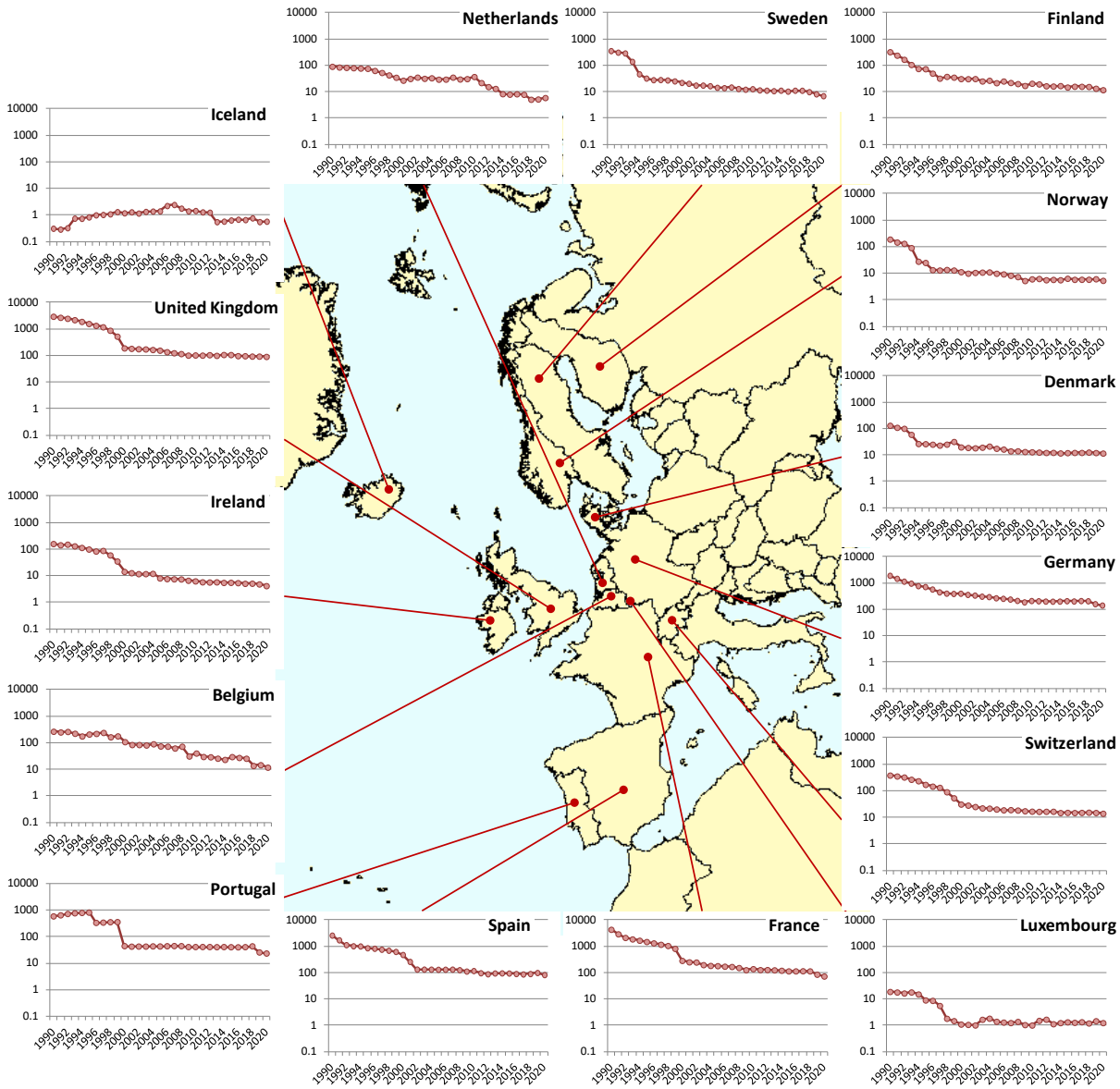

Fig. 2. *Time series of Pb emissions from the OSPAR Contracting Parties. Units: t/y.*

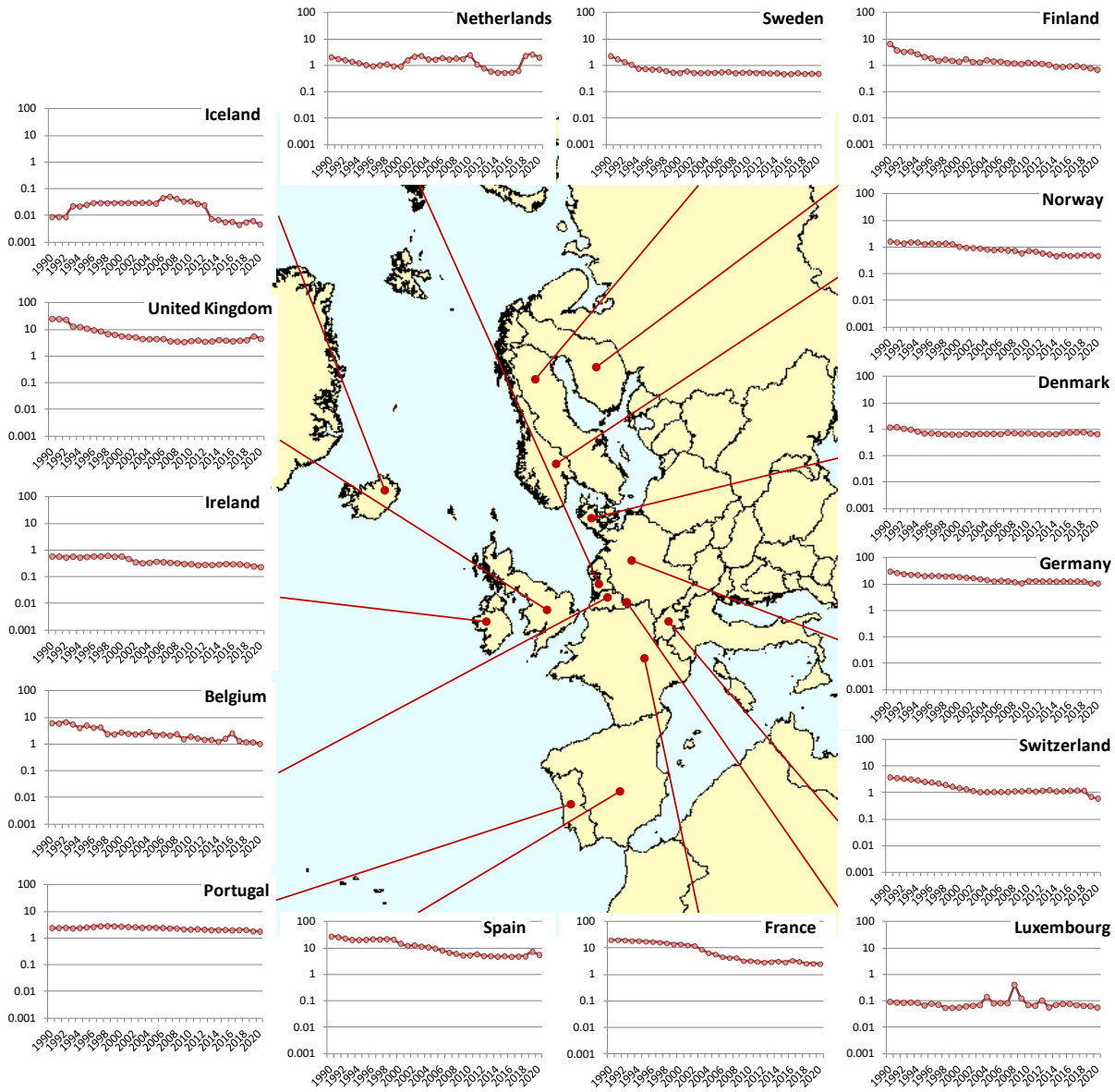

Fig. 3. *Time series of Cd emissions from the OSPAR Contracting Parties. Units: t/y.*

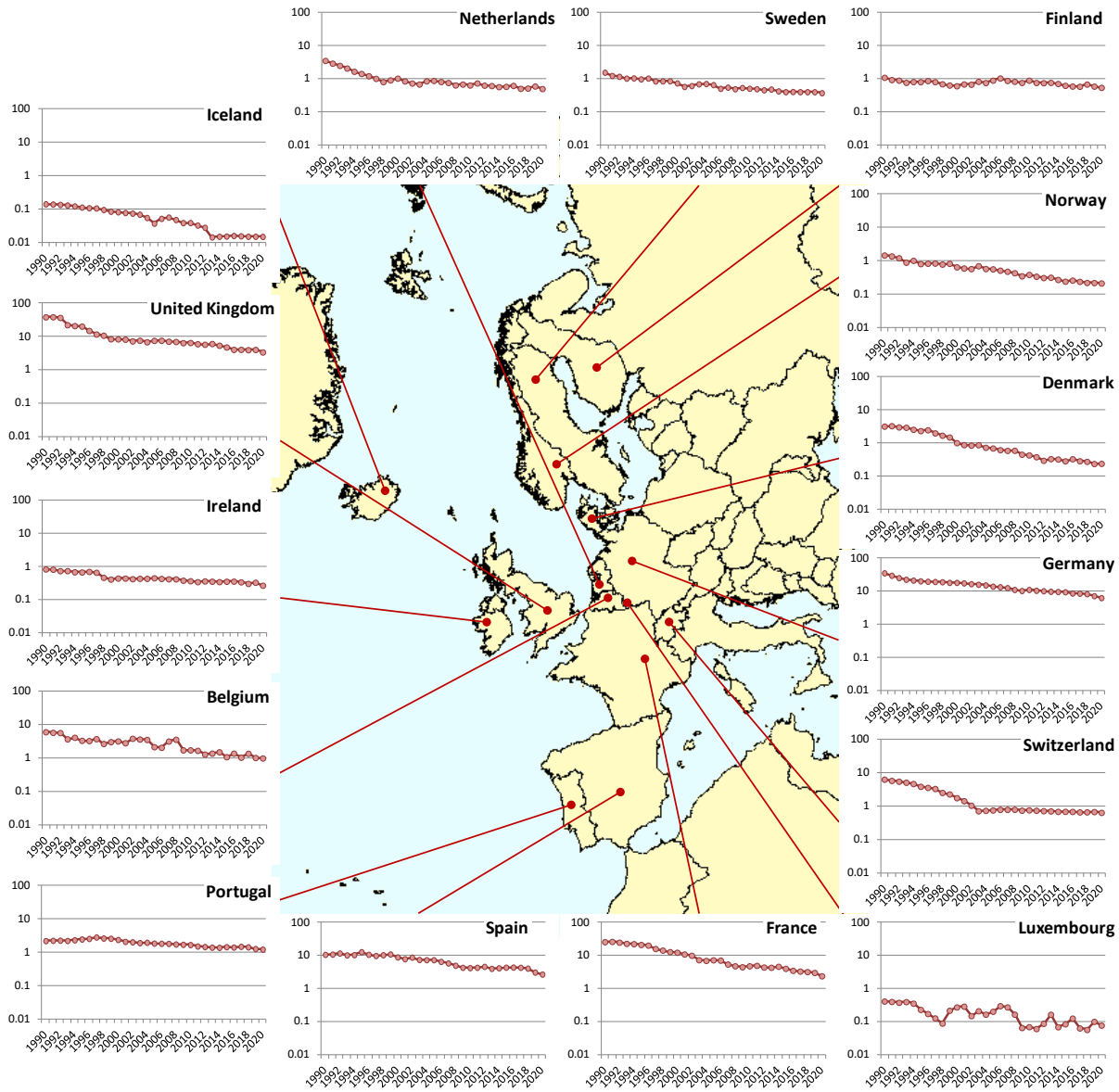

Fig. 4. *Time series of Hg emissions from the OSPAR Contracting Parties. Units: t/y.*

The contributions of individual sectors differed markedly among the countries. The sector B_Industry prevailed in Belgium, Finland, the Netherlands, Portugal, Spain and Sweden, where its contribution to national total emissions ranged from 54% to 63% (Fig. 5). Besides, substantial contribution (24% – 49%) of this sector was noted for France, Germany, Luxembourg, Norway and the United Kingdom. Fraction of the sector F_RoadTansport to total emissions varied from 20% to 45% in Denmark, France, Germany, Ireland, Luxembourg, Norway, Portugal, Spain and the United Kingdom. Sweden, Finland, Luxembourg and Switzerland were characterized by significant (12% – 28%) role of emissions from the sector A_PublicPower. The sector C_OtherStatComb made up considerable contribution to Pb emission in Ireland (44%) as well as Germany, Finland, Norway, France and Sweden (10% – 16%). In Iceland about 2/3 of national emissions were caused by the sector E_Solvents. In Switzerland large contribution (about 40%) was made by the sector M_Other. According to national Informative

Inventory Report, this sector included fires in buildings and emissions due to damage of motor vehicles [*Bass et al.,* 2022].

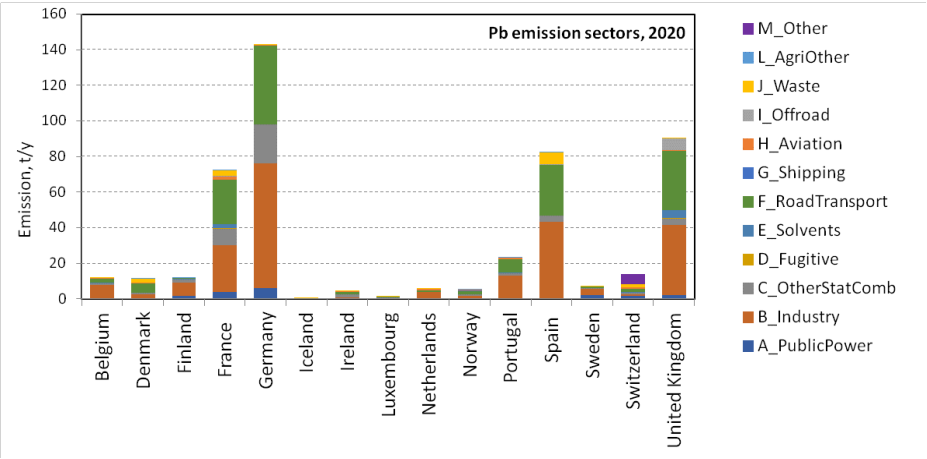

Fig. 5. *Emission of Pb from GNFR sectors in the OSPAR Contracting Parties in 2020.*

The main contribution to Cd emissions in the OSPAR Contracting Parties was made by the sector B_Industry (58%), followed by C_OtherStatComb (14%) and E_Solvents (11%) (Table A.7). Emissions from the Industry sector were presented mostly by production of copper, iron, steel and zinc. Another important activity was stationary combustion in manufacturing industries and construction. Altogether these activities contributed 70% to total OSPAR emission in this sector (Table A.9). GNFR sector C_OtherStatComb was presented by NFR sectors 'Commercial/Institutional: Stationary' and 'Residential: Stationary', which joint contribution was 95%. Predominant (99%) activity of the sector E_Solvents was formulated as 'Other product use'.

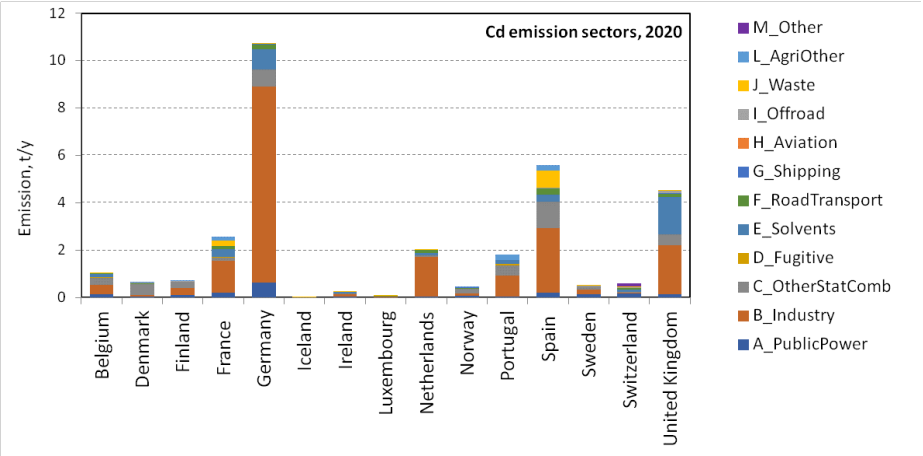

Fig. 6. *Emission of Cd from GNFR sectors in the OSPAR Contracting Parties in 2020.*

The sector B_Industry was predominant in Germany, France and the Netherlands, contributing more than 50% to total national emissions (Fig. 6). Its role was significant also in Belgium, Finland, Iceland, Ireland, Luxembourg, Norway, Portugal, Spain and the United Kingdom, where its contribution ranged from 24% to almost 50% of national total emission. Only in Switzerland and Denmark its contribution was relatively low amounting to around 10%. The sector C_OtherStatComb was the

major source of emissions in Denmark (almost 70%). Besides, in Belgium, Finland, Norway, Portugal, Spain and Sweden its contribution varied from 20% to almost 40%. The highest contribution of the sector E_Solvents to national total Cd emission took place in the United Kingdom (35%), followed by Ireland (21%) and Iceland (16%). In other countries its contribution ranged from 0.3% to 13%. In Sweden, Finland, Belgium, Ireland, Luxembourg, Norway and Switzerland substantial contribution (around 10 – 30%) was made by the sector A_PublicPower. In addition, sector I_OffRoad contributed almost 40% to emissions in Iceland, sector J_Waste provided 12% of national emission in Spain and sector M_Other was responsible for 24% of Cd emission in Switzerland.

Main contributors to Hg emissions in the OSPAR Contracting Parties were the sectors B_Industry (46%), A_PublicPower (29%) and J_Waste (8%). The sectors C_OtherStatComb and F_RoadTransport contributed around 6% each to the emission. The input of other sectors was insignificant (Table A.8). The only activity composing sector A_PublicPower was production of public electricity and heat (Table A.9). The main activities of the industry sector were iron, steel and cement production, and stationary combustion in various manufacturing industries and construction. These activities added up almost 70% to emissions in sector B_Industry. The main activity of the sector J_Waste was cremation. Other important activities were biological treatment of waste and sewage sludge incineration. These activities were responsible for 87% of the waste sector emissions.

Contribution of emission sectors to national emissions varied considerably among the OSPAR countries. In Belgium, Finland, France, Luxembourg, the Netherlands, Portugal and Spain the fraction of the sector B_Industry in national total emission exceeded 50% (Fig. 7). Besides, its contribution was substantial (22% - 43%) in Denmark, Germany, Ireland, Norway, Sweden, Switzerland and the United Kingdom. About one half of Hg emissions in Germany were caused by the sector A_PublicPower. Besides, in Denmark, Finland, France, Ireland, Sweden, Switzerland and the United Kingdom the contribution of this sector was also significant (21% – 47%). In Iceland the sector J_Waste provided more than 50% of national emission. Moreover, relatively high contribution of this sector was noted for the United Kingdom, Ireland, France, Spain and Sweden (9% – 24%). The largest contribution of the sector C_OtherStatComb took place in Ireland (30%), and the sector F_RoadTransport in the Netherlands (18%).

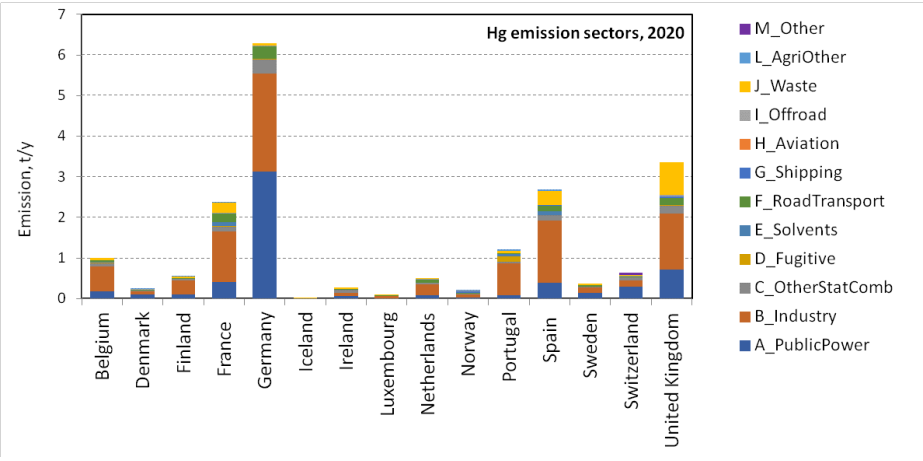

Fig. 7. *Emission of Hg from GNFR sectors in the OSPAR Contracting Parties in 2020.*

4. Deposition of Pb, Cd and Hg in 2020 and their trends

4.1. Lead

Total deposition flux of lead ranged from 0.05 to 0.5 kg/km^2/y over the most part of the OSPAR maritime area (Fig. 8). The highest fluxes (0.3 – 0.5 kg/km^2/y) were noted for the eastern part of the Region II (Greater North Sea). It was caused by a combination of factors such as atmospheric transport from land areas with significant anthropogenic and secondary sources (e.g., wind re-suspension of soil and dust particles, or suspension of sea spray aerosols containing natural and legacy trace metals) and high atmospheric precipitation. Significant annual precipitation sums also led to relatively high deposition over the northern part of Region V (Wider Atlantic) and the southern part of Region I (Arctic Waters). The lowest deposition levels took place in the southern part of Region V and the northern part of Region I due to their remoteness from the main emission regions and relatively low atmospheric precipitation. The highest spatial mean Pb deposition flux took place in Region II (0.29 kg/km^2/y), and the lowest - in Region I (0.14 kg/km^2/y) (Table A.10). Mean fluxes to Regions III, IV and V were 0.26, 0.18 and 0.20 kg/km^2/y, respectively.

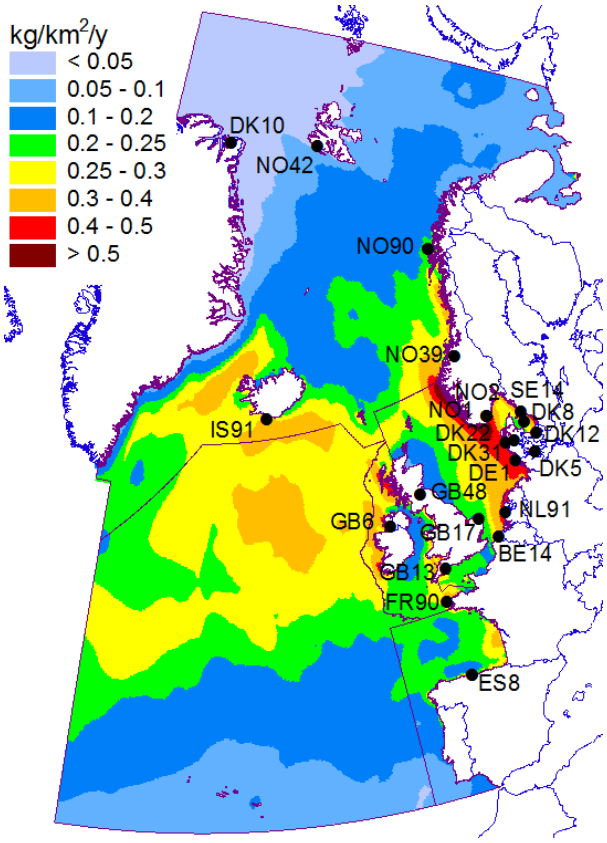

Fig. 8. *Spatial distribution of annual Pb deposition flux to the OSPAR maritime area in 2020. Purple lines depict borders of the OSPAR regions.*

Modelled time series of atmospheric Pb deposition to the OSPAR regions and their approximated trends are presented in Fig. 9. Following the decline of Pb emissions in Europe, the deposition fluxes exhibited long-term decrease from 1990 to 2020. The highest decrease (87%) was obtained for Region II (Greater North Sea), followed by 83% in Region IV (Bay of Biscay and Iberian Coast) and 80% in Region III (Celtic Seas). The lowest decline was noted for the Regions I and V (56% and 54%, respectively). Regions II, III and IV are located close to main emission regions. Therefore, their response to the reduction of emissions was stronger compared to that in Regions I and V. The existence of declining trend in modelled deposition at 0.001 significance level was revealed using Mann-Kendall test. The strongest reduction of deposition (3.6 – 9.5 % per year) took place in the first third of the considered period. The rate of reduction between 1990 and 2000 was substantially higher than that in the period from 2001 to 2020 (1.5 – 4.8 % per year) (Fig. 10). The difference in

deposition reduction rates is manly explained by the fact that emissions in the beginning of the considered period had been reducing stronger than in the other part of the period (Fig. 2 - 4).

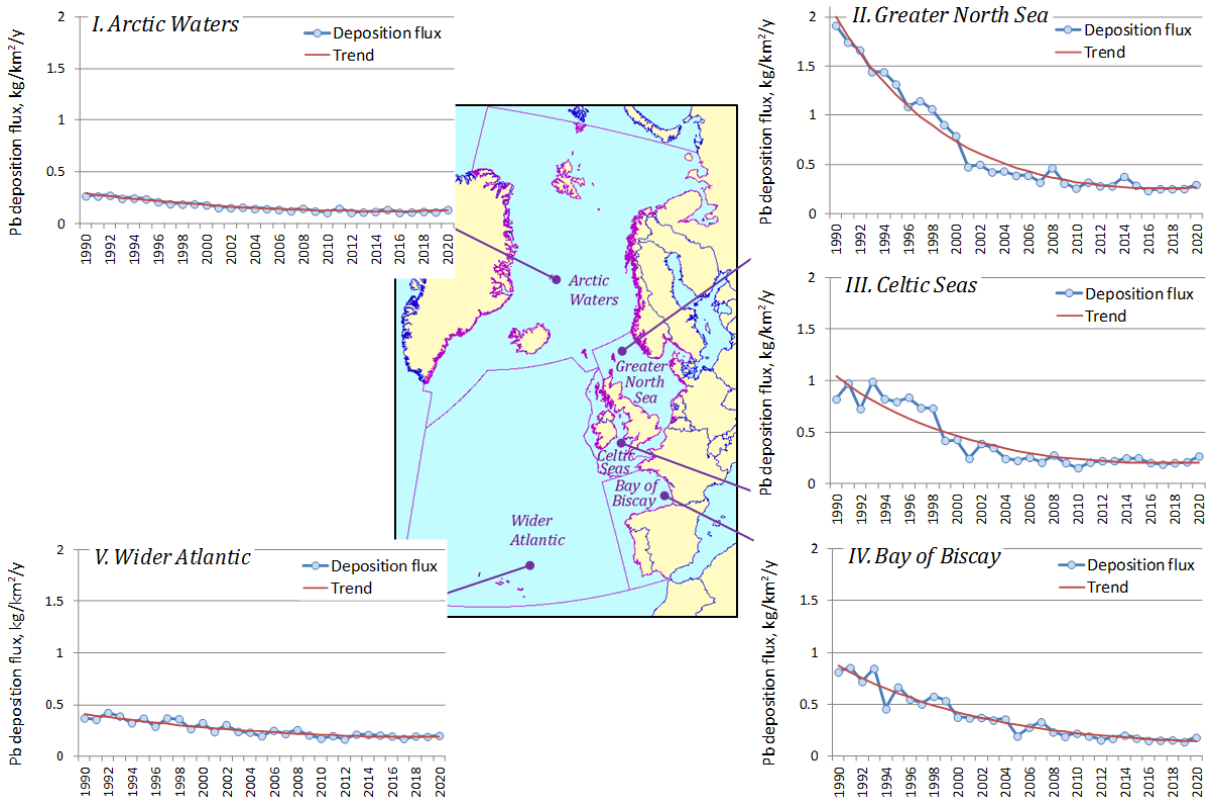

Fig. 9. *Time series of average annual Pb deposition flux to five regions of the OSPAR maritime area in the period 1990-2020. Blue line is the model estimate, red line is trend approximation.*

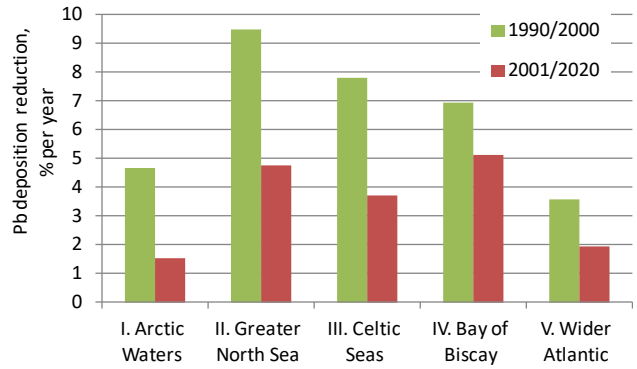

Fig. 10. *Mean rate of Pb deposition reduction (% per year) in the periods 1990-2000 and 2001-2020 in the OSPAR regions.*

4.2. Cadmium

Spatial distribution of Cd deposition flux in 2020 is similar to that of Pb (Fig. 11). The highest fluxes ranging from 10 to 15 g/km^2/y took place in the eastern part of Region II (Greater North Sea). Deposition flux in Region III (Celtic Seas) reached 15 g/km^2/y along the western coasts of Ireland and the United Kingdom and in the south-western part of Region I (Arctic Waters). Relatively high deposition fluxes (8 – 12 g/km^2/y) were also noted for the northern part of Region V (Wider Atlantic) due to significant precipitation amount. Relatively low deposition (< 3 g/km^2/y) took place in the northern part of Region I and the southern part of Region V. The highest spatial mean flux of Cd was noted for Region II (10.3 g/km^2/y), and the lowest- for Region I (5.1 g/km^2/y) (Tale A.11). In Regions III, IV and V the corresponding fluxes were 9.1, 5.9 and 6.7 g/km^2/y.

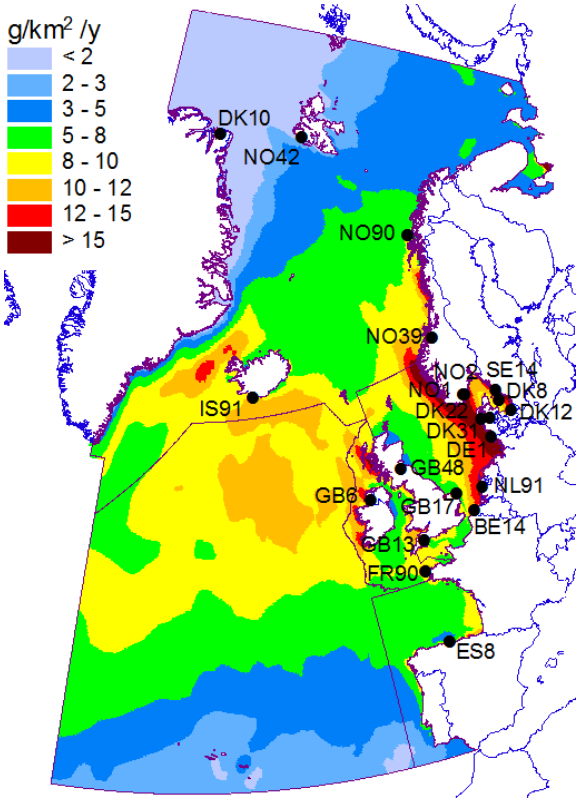

Fig. 11. *Spatial distribution of annual Cd deposition flux to the OSPAR maritime area in 2020. Purple lines depict borders of the OSPAR regions.*

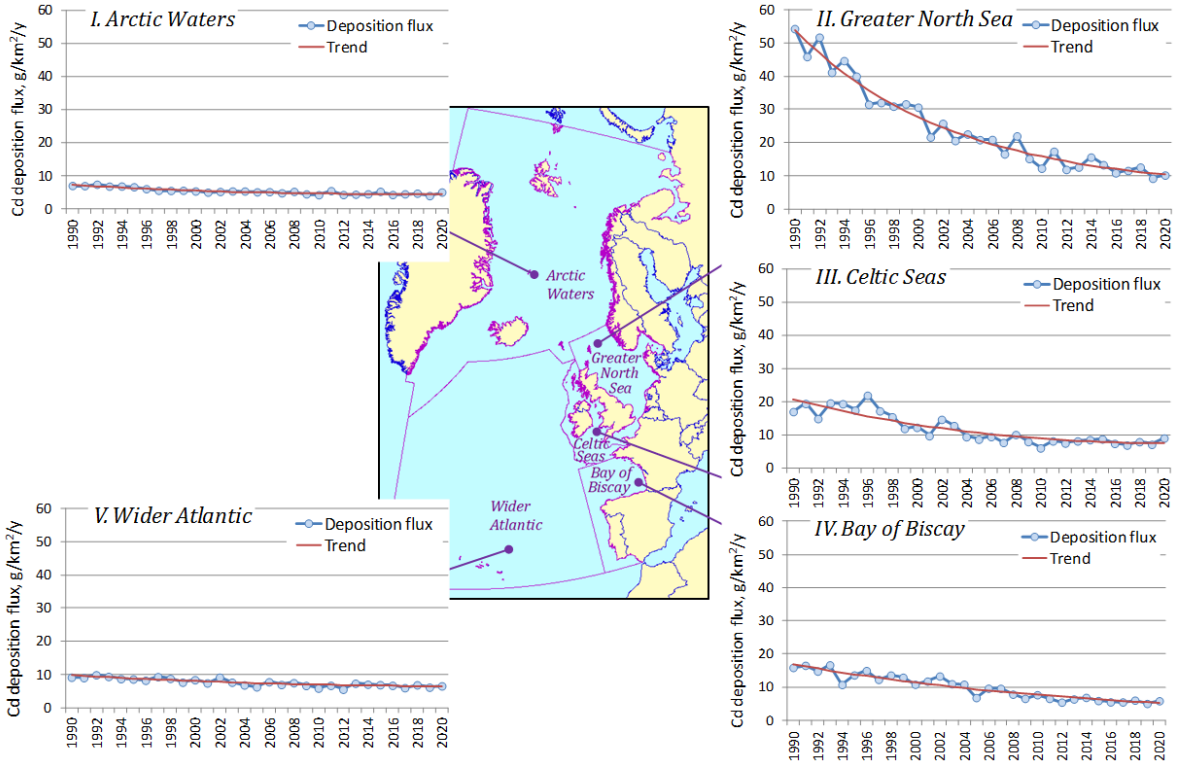

***Fig. 12**. Time series of average annual Cd deposition flux to five regions of the OSPAR maritime area in the period 1990-2020. Blue line is the model estimate, red line is trend approximation.*

Reduction of Cd deposition for the period from 1990 to 2020 varied markedly for the OSPAR regions. The highest decline (81%) was noted for Region II, followed by Region IV (69%) and Region III (63%) (Fig. 12). Regions I and V were characterized by the lowest reduction of Cd deposition amounting to 38% and 34%, respectively. Regions II, III and IV are located close to mainland-based emission sources of Cd. Therefore, the decline of emissions in Europe had stronger effect on deposition to these regions compared to more remote Regions I and V. The declining deposition trends were identified with significance level of 0.001 using Mann-Kendall test. The highest mean rate of deposition reduction was estimated for the first decade of the considered period, ranging from 1.9 to 6.4% per year (Fig. 13). In the remaining part of the period the mean reduction rate of deposition was 0.8 – 4.7 % per year.

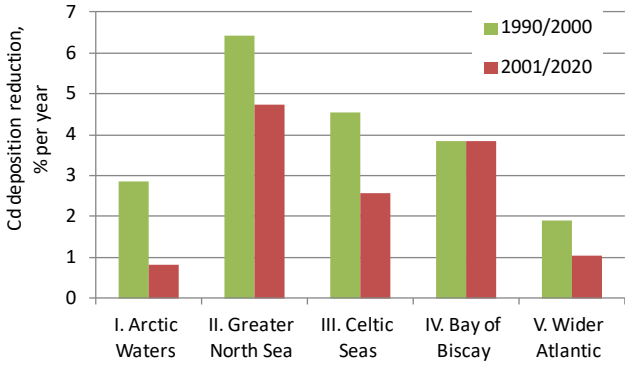

***Fig. 13.** Mean rate of Cd deposition reduction (% per year) in the periods 1990-2000 and 2001-2020 in the OSPAR regions.*

4.3. Mercury

Over most part of the OSPAR maritime area annual deposition fluxes of mercury varied from 4 to 17 g/km^2/y (Fig. 14). In the eastern part of the Region I (Arctic Waters) the fluxes exceeded 15 g/km^2/y. The reason for this is significant deposition of Hg due to springtime Arctic Mercury Depletion Events (AMDEs) [*Steffen et al.*, 2008]. However, it should be taken into account that large part of Hg deposited to snow or ice during AMDEs is photoreduced to its elemental form and re-emits to the atmosphere [*Moore et al.*, 2014; *Wang et al.,* 2019]. Elevated levels of Hg deposition (10 – 15 g/km^2/y) also took place in the western part of the Region I (Arctic Waters) in Denmark Strait and

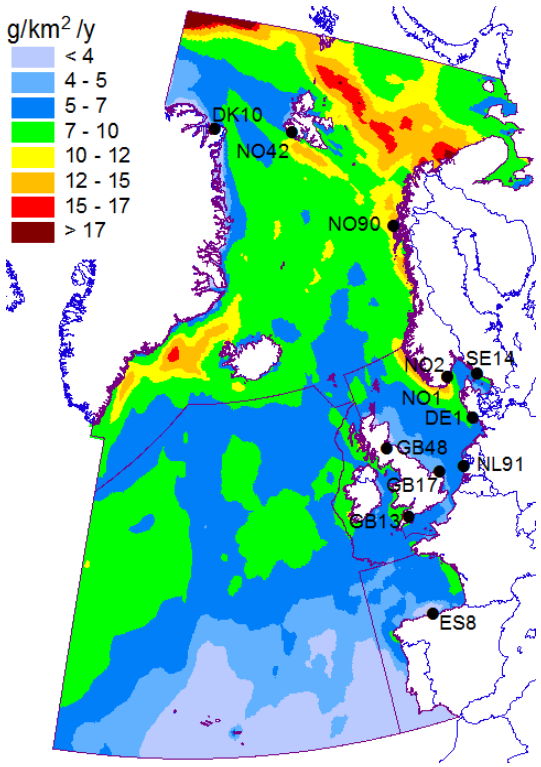

***Fig. 14.** Spatial distribution of annual Hg deposition flux to the OSPAR maritime area in 2020. Purple lines depict borders of the OSPAR regions.*

along the western coast of the Scandinavian Peninsula because of high precipitation. The lowest levels were noted in the southern part of Regions V (Wider Atlantic) and IV (Iberian Coast) due to low atmospheric precipitation. Region I is characterized by the highest spatial mean Hg deposition flux (8.9 g/km^2/y) (Table A.12). The lowest flux is noted for Region IV (4.8 g/km^2/y). Mean deposition fluxes to Regions II, III and V were equal to 6.6, 6.7 and 5.9 g/km^2/y, respectively. Compared to Pb and Cd, reduction of Hg deposition to the OSPAR regions for 1990-2020 was relatively low ranging from 19% in Region V (Wider Atlantic) to almost 50% in Region II (Greater North Sea). Reductions in Regions I, III and IV made up 22%, 33% and 28%, respectively. Lower deposition decline, compared to Pb and Cd, is explained by significant contribution of intercontinental transport to Hg deposition in the OSPAR maritime area (Fig. 15). Declining trends of Hg deposition were identified at 0.001 significance level. Similar to Pb and Cd, rate of deposition reduction in the first decade of the considered period was higher than the rate after 2000. In particular, the mean rate of Hg deposition reduction from 1990 to 2000 ranged from 0.9 to 3.8 % per year, while in the period from 2001 to 2020 it was 0.5 – 1.4 % per year (Fig. 16).

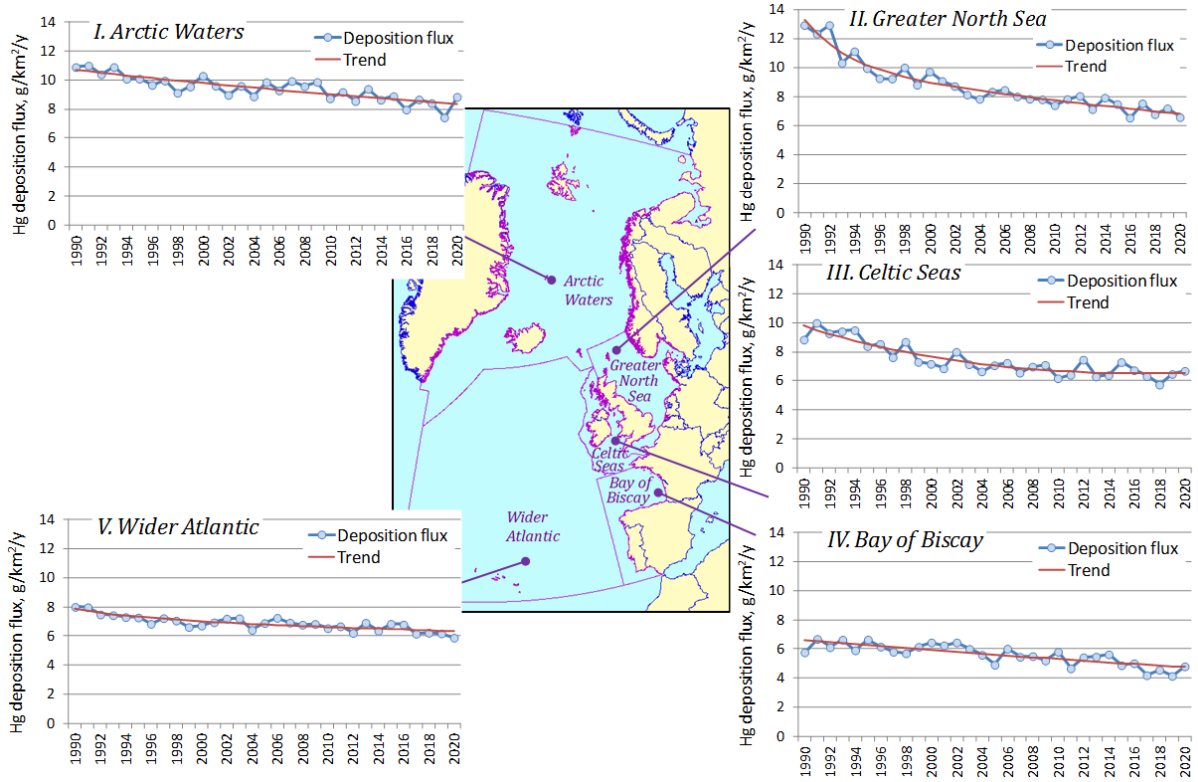

Fig. 15. *Time series of average annual Hg deposition flux to five regions of the OSPAR maritime area in the period 1990-2020. Blue line is the model estimate, red line is trend approximation.*

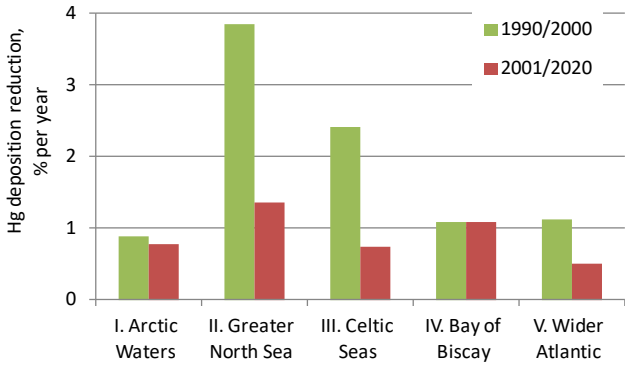

Fig. 16. *Mean rate of Hg deposition reduction (% per year) in the periods 1990-2000 and 2001-2020 in the OSPAR regions.*

5. Comparison of modelled and observed pollution levels in 2020

Comparison of modelled and observed air concentrations and wet deposition in 2020 was carried out for stations of Comprehensive Atmospheric Monitoring Programme (CAMP). The aim of the comparison is to evaluate the ability of the model to reproduce real pollution levels. Discrepancies between the modelled and observed concentrations or wet deposition fluxes can be caused by various reasons including uncertainties of emissions, modelling approaches and measurement data. Overview of these uncertainties is given in [*Ilyin et al.,* 2022]. It was concluded that the results of model were in satisfactory agreement with the available measurements and discrepancies did not exceed on average a factor of two.

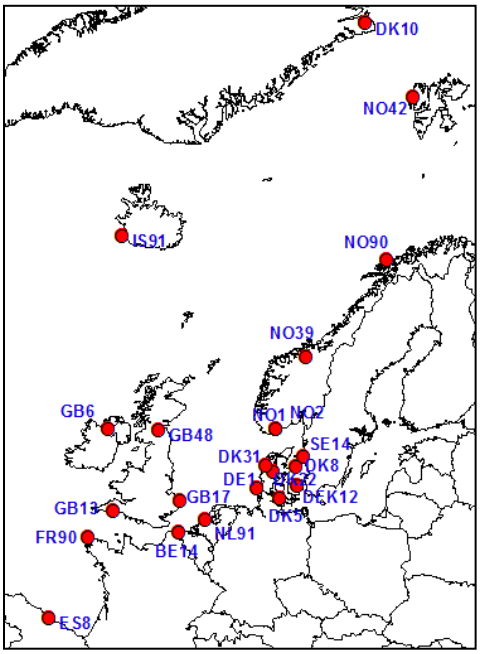

Fig. 17. *Location of stations of Comprehensive Atmospheric Monitoring Programme (CAMP) in 2020.*

There were totally 22 CAMP stations reporting concentrations in air or wet deposition fluxes of Pb, Cd and Hg in 2020 (Fig. 17). Modelled and observed annual mean values at CAMP stations in 2020 are summarized in Annex B. Measured Pb air concentrations were available at 14 CAMP stations (Fig. 18a). On average, the model tended to overestimate air concentrations by about factor 1.6, especially at stations in Belgium, Germany, Denmark, Sweden and one Norwegian site (Fig. 18a). Most likely, the overestimation is caused by overestimated contribution of secondary emission sources. Overestimation of the Icelandic station is related to the improvements in quality of measurements in this country, which led to significant decrease of the observed levels after 2015. At the British stations and Norwegian station NO2 the overestimation was moderate. On average, at 70% of the stations the difference between modelled and observed concentrations was within a factor of two.

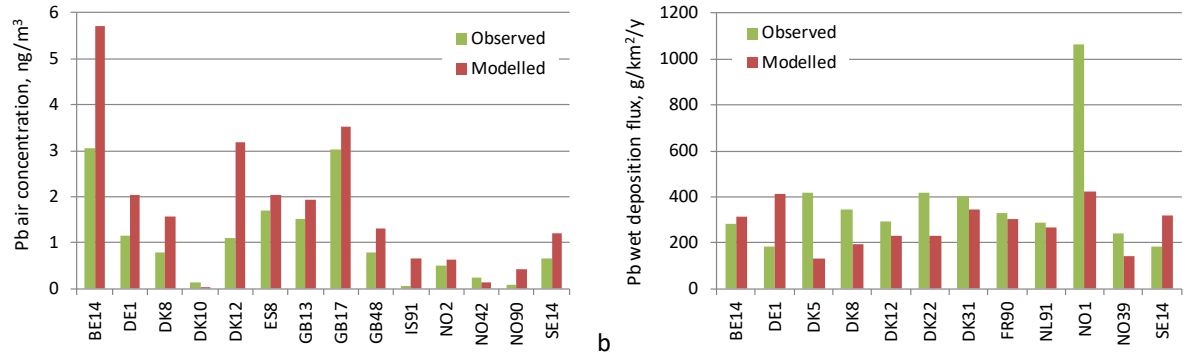

Fig. 18. *Modelled and observed mean annual Pb concentrations in air (a) and annual wet deposition fluxes (b) at the CAMP monitoring stations in 2020.*

Wet deposition fluxes in 2020 were observed at 17 CAMP stations. However, the results from four British stations were not used in the comparison because most of the sampled values were below detection limits or contaminated. Besides, for station ES8 the model underestimated wet deposition fluxes by factors 11. The flux at the ES8 station is the highest among the observed values at the EMEP stations. Since it is very unlikely that this high discrepancy can be explained entirely by uncertainties of the model, the results for these stations were removed from the analysis.. However, in Annex B the modelled and observed values for all stations are presented.

For the remaining stations the model demonstrated mean relative bias of -26%. Therefore, on average deposition fluxes of Pb to the CAMP stations were somewhat underestimated by the model. For 75% of stations the modelled and observed wet deposition fluxes agreed within a factor of two (Fig. 18b). At stations DE1 and DK5 the model overestimated the observed fluxes by factor 2.3 and 3.1, respectively. Most likely, the reason of the discrepancy is overestimated contribution of secondary sources for these stations. For the Norwegian station the model underestimated the observed flux by factor 2.5. On one hand, observed high wet deposition flux was correlated with high precipitation sum. On the other hand, observed concentration of Pb in precipitation at this station was also the highest among the CAMP stations. These high Pb levels, compared to other CAMP stations, could be explained by uncertainties of emissions or measurements. In particular, some samples in raw data from this station were marked as contaminated.

Concentrations of Cd in air in 2020 were measured at 14 CAMP stations. The model tended to overpredict observed concentrations in air on average by 70% (Fig. 19). Analysis of contributions of emission sources to modelled air concentration showed that at a number of stations even anthropogenic component of modelled concentrations in air exceeded the observed value. Therefore, the discrepancies could be caused by uncertainties of emission data or their vertical dispersion. For the Arctic station NO42 the model underestimated the observed concentrations by an order of magnitude. However, it is worth noting that the observed Cd level at this remote station is comparable with that measured in areas located closer to emission sources, e.g., Belgium, Germany, Denmark and the United Kingdom. These high air concentrations at the remote Arctic station could likely be explained by either unaccounted (e.g., local) emission sources or uncertainties of measurements.

Data on Cd wet deposition fluxes in 2020 were available from 17 CAMP stations. Similar to Pb, the data from four British stations were not used in the analysis because of large number of samples below detection limit or contamination. Besides, for Spanish station ES8 the 17-fold deviation between modelled and observed flux was indicated. This large discrepancy cannot be explained by the model uncertainties and require special research. Among the CAMP stations Cd wet deposition flux at ES8 is the highest. Therefore, the results of this station were not included in the analysis. In Annex B the modelled and observed values for all stations are presented. Mean relative bias for the remaining stations was -42% indicating some underestimation of the observed levels (Fig. 19b). For about 40% of stations modelled and observed wet deposition fluxes agree within a factor of two. For stations FR90, SE14 and Danish stations the modelled fluxes exceed the observed values by factor 2.1 – 2.5. It can be associated with the uncertainties of emissions, the model and measurements.

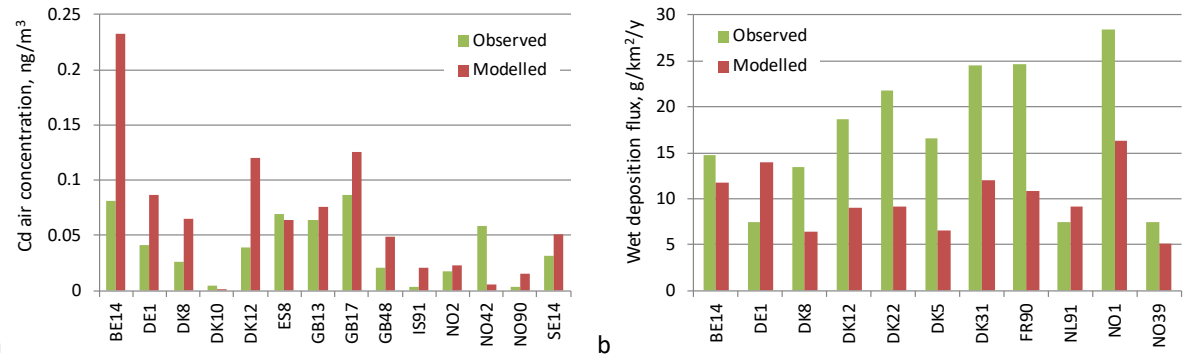

Fig. 19. *Modelled and observed mean annual Cd concentrations in air (a) and annual wet deposition fluxes (b) at the CAMP monitoring stations in 2020.*

Concentrations of Hg in air were available from 7 CAMP monitoring stations. Annual mean concentrations at Spanish station ES8 were unrealistically low (about 0.4 ng/m^3) and were not used in the evaluation of the modelling results. For other stations mean observed and modelled Hg concentration in air were 1.40 ng/m^3 and 1.26 ng/m^3, respectively (Fig. 20a). Relative difference between modelled and observed concentrations at most of stations varied from -15% to 6%, and mean relative bias was about -10%.

Wet deposition fluxes of Hg in 2020 were reported by 8 CAMP stations. Mean relative bias was about 16% indicating some overestimation of the observed values (Fig. 20b). At most of the stations relative bias between the observed and modelled values lied within ±50%. Annual modelled and observed wet deposition fluxes agreed within factor of two for all the stations. Some overestimation (50 – 80%) was noted for stations DE1, GB48 and SE14. At station NL91 the model underestimated observed wet deposition flux. The discrepancies between modelled and observed Hg wet deposition fluxes can mainly be explained by uncertainties of Hg chemistry and uncertainties of Hg speciation of anthropogenic emissions.

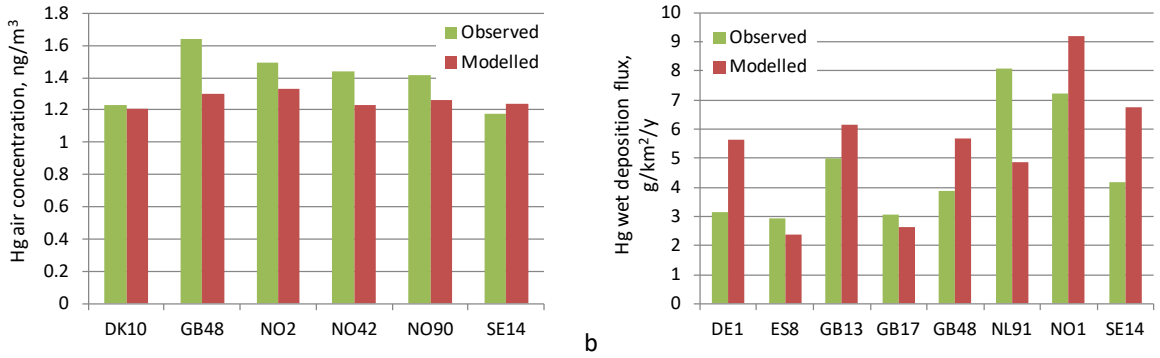

***Fig. 20**. Modelled and observed mean annual Hg concentrations in air (a) and annual wet deposition fluxes (b) at the CAMP monitoring stations in 2020.*

In general, discrepancies between the modelled and observed concentrations in air and wet deposition fluxes of Pb, Cd and Hg can be explained by a number of factors including uncertainties of emission data, measurements and the modelling approaches. According to officially reported uncertainties of heavy metal emissions in the OSPAR Contracting Parties made up 25 - 480% for Pb, 30 - 360% for Cd and 30 - 110% for Hg [*CEIP*, 2022]. Besides, estimates of secondary emissions are also subject to significant uncertainties. Laboratory intercomparison tests demonstrated that the deviation between measured and theoretical concentrations of Pb or Cd in precipitation was better than 25% for the EMEP/CAMP laboratories [*CCC*, 2021]. However, these tests provide only analytical component of the uncertainties of measurement data. Other sources of the uncertainties (sampling, storing, shipping etc.) remain unaccounted. Uncertainties of the model have been evaluated by a number of model intercomparison studies [*Gusev et al.*, 2000; *Ryaboshapko et al.*, 2001, 2005] as well as during the thorough model review under supervision of the EMEP Task Force of Measurements and Modelling (TFMM) [ECE/EB.AIR/GE.1/2006/4]. It was concluded that the results of the model were in satisfactory agreement with the available measurements and discrepancies did not exceed on average a factor of two.

6. Conclusions

Assessment of atmospheric pollution of the OSPAR maritime area by Pb, Cd and Hg in 2020 was carried. Long-term time series of atmospheric emissions in the OSPAR Contracting Parties and deposition to five OSPAR regions for the period 1990-2019 were updated by the values for 2020 and analyzed. Deposition fluxes to the OSPAR maritime area were simulated using atmospheric transport model. Modelled concentrations in air and wet deposition fluxes were compared with the available data reported from stations of the CAMP monitoring programme. The main outcomes of the study are summarized below.

1. Total Pb, Cd and Hg emission in the OSPAR Contracting Parties in 2020 amounted to 483, 32 and 20 tonnes, respectively. The highest emissions were noted for Germany, the United Kingdom, Spain and France. Their contribution to total OSPAR emission was 80% for Pb and 74% for Cd and Hg in 2020. Reduction of Pb, Cd and Hg atmospheric emissions in the OSPAR Contracting Parties from 1990 to 2020 was 97%, 76% and 86%, respectively. The highest reduction of Pb is noted for France and Sweden (98% each). Finland is known for the most significant (90%) decrease of Cd emission. The highest reduction of Hg mission was reached in Denmark (93%). Emissions of Pb, Cd and Hg are characterized by stronger rate of reduction in the first decade of the considered period compared to the reduction from 2000 to 2020.

2. Contributions of Pb, Cd and Hg GNFR emission sectors to total emissions in the OSPAR Contracting Parties were analyzed. The main emission sectors contributing to the OSPAR Pb emission are B_Industry (45%), F_RoadTransport (32%) and C_OtherStatComb (10%). The main sector (B_Industry) prevails in Belgium, Finland, the Netherlands, Portugal, Spain and Sweden. The main contributor to Cd total emission is made by sector B_Industry (58%), followed by C_OtherStatComb (14%) and E_Solvents(11%). The sector B_Industry is predominant in Germany, France and the Netherlands, contributing more than 50% to total national emissions. Sectors B_Industry (46%) and A_PublicPower(29%) are the main contributors to total Hg emissions in the OSPAR countries. Fraction of sector B_Industry in national total emission exceeds 50% in Belgium, Finland, France, Luxembourg, the Netherlands, Portugal and Spain.

3. The highest spatial mean deposition fluxes of Pb (0.29 kg/km^2/y) and Cd (10.3 g/km^2/y) in 2020 were noted for Region II. The lowest fluxes (0.14 kg/km^2/y and 5.1 g/km2/y, respectively) took place in Region I. In case of Hg, Region I is characterized by the highest (8.9 g/km^2/y), and Region IV - by the lowest (4.8 g/km^2/y) spatial mean deposition flux.

4. Deposition of Pb, Cd and Hg to the OSPAR maritime area substantially declined from 1990 to 2020. The highest decline of Pb, Cd and Hg deposition took place in Region II (Greater North Sea) and amounted to 87%, 81% and almost 50%, respectively. The lowest decline of deposition is noted for Region I (Arctic Waters) and Region V (Wider Atlantic), amounting to about 55% for Pb, about 35% - 40% for Cd and around 20% for Hg. The decline of deposition to the OSPAR regions is lower than the emission reduction because of the effect of secondary and global sources.

Existence of long-term declining deposition trends was confirmed by Mann-Kendall test at 0.001 level of significance.

5. Modelled concentrations in air and wet deposition fluxes were compared with the data from CAMP monitoring stations. The model tends to somewhat overestimate observed concentrations of Pb and Cd and air. Wet deposition fluxes of Pb were reproduced with relatively low mean relative bias (-26%. For the majority of stations the modelled and observed concentrations and deposition fluxes agree within a factor of two. Wet deposition fluxes of Cd were underestimated by about 40% at the CAMP stations. The agreement between modelled and observed Hg concentrations in air is within ±15% at most of stations. Mean relative bias for Hg wet deposition fluxes is 16%.

References

Bain L. and Engelhardt M. [1992] Introduction to probability and mathematical statistics. 2nd ed., Duxbury.

Bass A.A., Guillevic M., Kegel R., Leuenberger D., Müller B. and Schneker S. [2022]. Switzerland's Informative Inventory Report 2022. Submission of March 2022 to the United Nations ECE Secretariat. Federal Office for the Environment FOEN. 434 p.

CCC [2021] EMEP laboratory intercomparison. Heavy metals in precipitation 2020 - % deviation from expected value. https://projects.nilu.no/ccc/intercomparison/index.html . Site visited 09.06.2021.

CEIP [2022]. EMEP Centre on Emission Inventories and Projections. Status of reporting. https://www.ceip.at/status-of-reporting-and-review-results/2022-submission. Visited 05.09.2022.

Colette A., Aas W., Banin L., Braban C.F., Ferm M., González Ortiz A., Ilyin I., Mar K., Pandolfi M., Putaud J.-P., Shatalov V., Solberg S., Spindler G., Tarasova O., Vana M., Adani M., Almodovar P., Berton E., Bessagnet B., Bohlin-Nizzetto P., Boruvkova J., Breivik K., Briganti G., Cappelletti A., Cuvelier K., Derwent R., D'Isidoro M., Fagerli H., Funk C., Garcia Vivanco M., González Ortiz A., Haeuber R., Hueglin C., Jenkins S., Kerr J., de Leeuw F., Lynch J., Manders A., Mircea M., Pay M.T., Pritula D., Putaud J.-P., Querol X., Raffort V., Reiss I., Roustan Y., Sauvage S., Scavo K., Simpson D., Smith R.I., Tang Y.S., Theobald M., Tørseth K., Tsyro S., van Pul A., Vidic S., Wallasch M., Wind P. [2016] Air pollution trends in the EMEP region between 1990 and 2012. Joint Report of the EMEP Task Force on Measurements and Modelling (TFMM), Chemical Co-ordinating Centre (CCC), Meteorological Synthesizing Centre-East (MSC-E), Meteorological Synthesizing Centre-West (MSC-W) EMEP: CCC-Report 1/2016. 105 p. Available at https://projects.nilu.no/ccc/reports.html.

ECHA [2013]. Support document for identification of cadmium as a substance of very high concern because of its CMR properties and because of its adverse effects nn kidney and bone tissues after prolonged exposure, which cause probable serious effects to human health which give rise to an equivalent level of concern to those of CMR and PBT/vPvB. 24 p.

ECHA [2018]. Support document for identification of lead (lead powder and lead massive) as a substance of very high concern because of its toxic for reproduction properties (article 57c). 7 p.

Emmons L.K., Walters S., Hess P.G., Lamarque J.-F., Pfister G.G., Fillmore D., Granier C., Guenther A., Kinnison D., Laepple T., Orlando J., Tie X., Tyndall G., Wiedinmyer C., Baughcum S.L., and Kloster S. [2010] Description and evaluation of the Model for Ozone and Related chemical Tracers, version 4 (MOZART-4), *Geosci. Model Dev*., 3, 43–67, doi:10.5194/gmd-3-43-2010.

Ferrari C. P. et al. [2008] Atmospheric mercury depletion event study in Ny-Alesund (Svalbard) in spring 2005. Deposition and transformation of Hg in surface snow during springtime. *Sci. Total Environ*. 397, 167–177.

Gheorghe S., Stoica C., Vasile G.G., Nita-Lazar M., Stanescu E. and Lucaciu I.E. [2017]. Metals Toxic Effects in Aquatic Ecosystems: Modulators of Water Quality. In: *Water Quality*. Ed. by Hlanganani Tutu, 428p., DOI: 10.5772/62562

Gilbert R. [1987]. Statistical Methods for Environmental Pollution Monitoring. Van Nostrand Reinhold Company, New York, ISBN 0-442-23050-8. 320 p. Guidebook [2019]. EMEP/EEA Air Pollutant Emission Inventory Guidebook 2019. [https://www.eea.europa.eu/publications/emep-eea-guidebook-2019].

Gusev A., Ilyin I., Mantseva L., Rozovskaya O., Shatalov V. and Travnikov O. [2006] Progress in further development of MSCE-HM and MSCE-POP models (implementation of the model review recommendations). EMEP/MSC-E Technical Report 4/2006.

Gusev A., O.Rozovskaya, V. Shatalov [2007] Modelling POP long-range transport and contamination levels by MSCE-POP model. EMEP/MSC-E Technical Report 1/2007.

Gusev A., Ilyin I., Petersen G., van Pul A. and Syrakov D. [2000] Long-range transport model intercomparison studies. Model intercomparison study for cadmium. EMEP/ESC-E Report 2/2000, Meteorological Synthesizing Centre – East, Moscow, Russia. (http://www.msceast.org/reports/2_2000.pdf).

Ilyin I., Rozovskaya O., Travnikov O., Aas W. and Pfaffhuber K.A. [2018] Assessment of heavy metal transboundary pollution on global, regional and national scales. EMEP Status Report 2/2018. 70 p.

Ilyin I., Travnikov O., Rozovskaya O. and I.Strizhkina [2022] Trends in deposition of heavy metals to the OSPAR maritime area. EMEP/MSC-E Technical Report 1/2022. 63 p.

Jin P., Zhang J., Wan J., Overmans S., Gao G., Ye M., Dai X., Zhao J., Xiao M. and Xia J. [2021] The Combined Effects of Ocean Acidification and Heavy Metals on Marine Organisms: A Meta-Analysis. Front. Mar. Sci. 8:801889. doi: 10.3389/fmars.2021.801889

Johnson K. P., Blum J. D., Keeler G. J. and Douglas T. A. [2008] Investigation of the deposition and emission of mercury in arctic snow during an atmospheric mercury depletion event. *J. Geophys. Res. Atmos*. 113, D17304.

Karcioglu O. and Arslan B. (Eds.) [2019] Poisoning in the Modern World - New Tricks for an Old Dog?. London, United Kingdom, IntechOpen, 2019 [Online]. Available from: https://www.intechopen.com/books/7111 doi: 10.5772/intechopen.73906.

Keller N., Stefani M., Einarsdóttir S.R., Helgadóttir A.K. and Helgason R. [2020] Informative Inventory Report. Emissions of air pollutants in Iceland from 1990 to 2018. The Environment Agency of Iceland. Publication ID: UST-2020:07. 200 p.

Kirk J. L., St Louis V. L. and Sharp M. J. [2006] Rapid reduction and reemission of mercury deposited into snowpacks during atmospheric mercury depletion events at Churchill, Manitoba, Canada. *Environ. Sci. Technol*. 40, 7590–7596.

Mitra S., Chakraborty A.J., Tareq A. M., Emran T.B., Nainu F., Khusro A., Idris A.M., Khandaker M.U., Osman H., Alhumaydhi F.A. and Simal-Gandara J. [2022] Impact of heavy metals on the environment and human health: Novel therapeutic insights to counter the toxicity. *Journal of King Saud University – Science* 34 (2022) 101865.

Moore C. W. et al. [2014] Convective forcing of mercury and ozone in the Arctic boundary layer induced by leads in sea ice. *Nature* 506, 81-84.

Naeem M., Ansari A.A. and Sarvajeet S.G. (Eds.) [2020] Contaminants in Agriculture. Sources, Impacts and Management. Springer Nature Switzerland AG 2020. , 445 p.

OSPAR [2017] Intermediate Assessment 2017. Available at: https://oap.ospar.org/en/ospar-assessments/intermediate-assessment-2017.

Rice K.M, Walker E.M., Miaozong J. Wu, Gillette C. and Blough E.R. [2014] Environmental Mercury and Its Toxic Effects . *J Prev Med Public Health* 2014; 47:74-83.

Richardson G.M., Garret R., Mitchell I., Mah-Paulson M. and T.Hackbarth [2001] Critical Review of natural global and regional emissions of six trace metals to the atmosphere. Final Report. Risklogic Scientific Services, Inc, 52p.+tables.

Ryaboshapko A., Artz R., Bullock R., Christensen J., Cohen M., Draxler R., Ilyin I., Munthe J., Pacyna J., Petersen G., Syrakov D., and Travnikov O. [2005] Itercopmparison study of numerical models for long-range atmospheric transport of mercury. Stage III. Comparison of modelling results with long-term observations and comparison of calculated itens of regional balances. EMEP/MSC-E Technical Report 1/2005, Meteorological Synthesizing Centre – East, Moscow, Russia. (http://www.msceast.org/reports/1_2005.pdf).

Ryaboshapko A., Ilyin I., Bullock R., Ebinghaus R., Lohman K., Munthe J., Petersen G., Seigneur C., Wangberg I. [2001] Intercomparison study of numerical models for long-range atmospheric transport of mercury. Stage I: Comparison of chemical modules for mercury transformations in a cloud/fog environment. EMEP/MSC-E Technical report 2/2001, Meteorological Synthesizing Centre – East, Moscow, Russia. (http://www.msceast.org/reports/2_2001.pdf).

Salminen R. (Chief-editor) [2005] Geochemical Atlas of Europe. Part 1 - Background Information, Methodology and Maps. A contribution to IUGS/IAGC Global Geochemical Baselines. ISBN 951-690-913-2 (electronic version). http://weppi.gtk.fi/publ/foregsatlas/index.php.

Shah S.B.[2021]. Heavy Metals in the Marine Environment—An Overview. In: Heavy Metals in Scleractinian Corals. *SpringerBriefs in Earth Sciences*. 90 p. doi:10.1007/978-3-030-73613-2.

Skamarock W.C., Klemp J.B., Dudhia J., Gill D.O., Barker D.M., Duda M.G., Huang X-Y., Wang W. and Powers J.G. [2008]. A Description of the Advanced Research WRF Version 3. NCAR/TN–475+STR NCAR TECHNICAL NOTE.

Steffen A. et al . [2008] A synthesis of atmospheric mercury depletion event chemistry in the atmosphere and snow. *Atmos. Chem. Phys*. 8, 1445-1482.

Tista M., Matthews B. and R.Wankmueller [2019] Methodologies applied to the CEIP GNFR gap -filling 2019. Part II: Heavy Metals (Pb, Cd, Hg) of the year 2017. Technical report CEIP 2/2019.

Travnikov O. and Ilyin I. [2009] "The EMEP/MSC-E mercury modelling system" in Mercury Fate and Transport in the Global Atmosphere, R. Mason, N. Pirrone, Eds. (Springer, Boston, MA, 2009), pp. 571–587.

UNECE [2012] 1998 Protocol on Heavy Metals, as amended on 13 December 2012. Executive Body for the Convention on Long-range Transboundary Air Pollution. 2012, http://www.unece.org/fileadmin/DAM/env/documents/2012/EB/ECE.EB.AIR.115_ENG.pdf.

Wang S. et al. [2019] Direct detection of atmospheric atomic bromine leading to mercury and ozone depletion. PNAS 116, 14479.

Wever D., Coenen P.W.H.G., Dröge R., Geilenkirchen G.P., Hoen M. 't., Honig E., Koch W.W.R., Leekstra A.J., Lagerwerf L.A., te Molder R.A.B., Peek C.J., Smeets W.L.M., Vonk J. and van de Zee T. [2020] Informative Inventory Report 2020. Emissions of transboundary air pollutants in the Netherlands 1990–2018. RIVM Report 2020-0032, 221 p.

Yang X., Cox R., Warwick N., Pyle J., Carver G., O'Connor F., and Savage N. [2005] Tropospheric bromine chemistry and its impacts on ozone: A model study, *J. Geophys. Res.,* 110, D23311, doi:10.1029/2005JD006244.

Yang X., Pyle J.A., Cox R.A., Theys N., and Van Roozendael M. [2010] Snow-sourced bromine and its implications for polar tropospheric ozone, *Atmos. Chem. Phys*., 10, 7763–7773, doi:10.5194/acp-10-7763-2010.

Annex A.

Data Products

Table A.1. *Codes of countries used in this study*

Name	Code	Name	Code
Belgium	BE	Netherlands	NL
Denmark	DK	Norway	NO
Finland	FI	Portugal	PT
France	FR	Spain	ES
Germany	DE	Sweden	SE
Iceland	IS	Switzerland	CH
Ireland	IE	United Kingdom	GB
Luxembourg	LU		

Table A.2. *List of emission sectors used in the EMEP emission reporting*

GNFR sector	NFR code	Description
A_PublicPower	1A1a	Public electricity and heat production
	1A1b	Petroleum refining
	1A1c	Manufacture of solid fuels and other energy industries
	1A2a	Stationary combustion in manufacturing industries and construction: Iron and steel
	1A2b	Stationary combustion in manufacturing industries and construction: Non-ferrous metals
	1A2c	Stationary combustion in manufacturing industries and construction: Chemicals
	1A2d	Stationary combustion in manufacturing industries and construction: Pulp, Paper and Print
	1A2e	Stationary combustion in manufacturing industries and construction: Food processing, beverages and tobacco
	1A2f	Stationary combustion in manufacturing industries and construction: Non-metallic minerals
	1A2gviii	Stationary combustion in manufacturing industries and construction: Other (please specify in the IIR)
	2A1	Cement production
	2A2	Lime production
	2A3	Glass production
	2A5a	Quarrying and mining of minerals other than coal
	2A5b	Construction and demolition
	2A5c	Storage, handling and transport of mineral products
	2A6	Other mineral products (please specify in the IIR)
B_Industry	2B1	Ammonia production
	2B2	Nitric acid production
	2B3	Adipic acid production
	2B5	Carbide production
	2B6	Titanium dioxide production
	2B7	Soda ash production
	2B10a	Chemical industry: Other (please specify in the IIR)
	2B10b	Storage, handling and transport of chemical products (please specify in the IIR)
	2C1	Iron and steel production
	2C2	Ferroalloys production
	2C3	Aluminium production
	2C4	Magnesium production
	2C5	Lead production
	2C6	Zinc production
	2C7a	Copper production
	2C7b	Nickel production
	2C7c	Other metal production (please specify in the IIR)
	2C7d	Storage, handling and transport of metal products (please specify in the IIR)

GNFR sector	NFR code	Description
	2D3b	Road paving with asphalt
	2D3c	Asphalt roofing
	2H1	Pulp and paper industry
	2H2	Food and beverages industry
	2H3	Other industrial processes (please specify in the IIR)
	2I	Wood processing
	2J	Production of POPs
	2K	Consumption of POPs and heavy metals (e.g. electrical and scientific equipment)
	2L	Other production, consumption, storage, transportation or handling of bulk products (please specify in the IIR)
C_OtherStationaryComb	1A4ai	Commercial/Institutional: Stationary
	1A4bi	Residential: Stationary
	1A4ci	Agriculture/Forestry/Fishing: Stationary
	1A5a	Other stationary (including military)
D_Fugitive	1B1a	Fugitive emission from solid fuels: Coal mining and handling
	1B1b	Fugitive emission from solid fuels: Solid fuel transformation
	1B1c	Other fugitive emissions from solid fuels
	1B2ai	Fugitive emissions oil: Exploration, production, transport
	1B2aiv	Fugitive emissions oil: Refining and storage
	1B2av	Distribution of oil products
	1B2b	Fugitive emissions from natural gas (exploration, production, processing, transmission, storage, distribution and other)
	1B2c	Venting and flaring (oil, gas, combined oil and gas)
	1B2d	Other fugitive emissions from energy production
E_Solvents	2D3a	Domestic solvent use including fungicides
	2D3d	Coating applications
	2D3e	Degreasing
	2D3f	Dry cleaning
	2D3g	Chemical products
	2D3h	Printing
	2D3i	Other solvent use (please specify in the IIR)
	2G	Other product use (please specify in the IIR)
F_RoadTransport	1A3bi	Road transport: Passenger cars
	1A3bii	Road transport: Light duty vehicles
	1A3biii	Road transport: Heavy duty vehicles and buses
	1A3biv	Road transport: Mopeds & motorcycles
	1A3bv	Road transport: Gasoline evaporation
	1A3bvi	Road transport: Automobile tyre and brake wear
	1A3bvii	Road transport: Automobile road abrasion
G_Shipping	1A3di(ii)	International inland waterways
	1A3dii	National navigation (shipping)
H_Aviation	1A3ai(i)	International aviation LTO (civil)
	1A3aii(i)	Domestic aviation LTO (civil)
I_Offroad	1A2gvii	Mobile combustion in manufacturing industries and construction (please specify in the IIR)
	1A3c	Railways
	1A3ei	Pipeline transport
	1A3eii	Other (please specify in the IIR)
	1A4aii	Commercial/Institutional: Mobile
	1A4bii	Residential: Household and gardening (mobile)
	1A4cii	Agriculture/Forestry/Fishing: Off-road vehicles and other machinery
	1A4ciii	Agriculture/Forestry/Fishing: National fishing
	1A5b	Other, Mobile (including military, land based and recreational boats)
J_Waste	5A	Biological treatment of waste - Solid waste disposal on land
	5B1	Biological treatment of waste - Composting
	5B2	Biological treatment of waste - Anaerobic digestion at biogas facilities
	5C1a	Municipal waste incineration
	5C1bi	Industrial waste incineration
	5C1bii	Hazardous waste incineration
	5C1biii	Clinical waste incineration
	5C1biv	Sewage sludge incineration

GNFR sector	NFR code	Description
	5C1bvi	Other waste incineration (please specify in the IIR)
	5C2	Open burning of waste
	5D1	Domestic wastewater handling
	5D2	Industrial wastewater handling
	5D3	Other wastewater handling
	5E	Other waste (please specify in the IIR)
K_AgriLivestock	3B1a	Manure management - Dairy cattle
	3B1b	Manure management - Non-dairy cattle
	3B2	Manure management - Sheep
	3B3	Manure management - Swine
	3B4a	Manure management - Buffalo
	3B4d	Manure management - Goats
	3B4e	Manure management - Horses
	3B4f	Manure management - Mules and asses
	3B4gi	Manure management - Laying hens
	3B4gii	Manure management - Broilers
	3B4giii	Manure management - Turkeys
	3B4giv	Manure management - Other poultry
	3B4h	Manure management - Other animals (please specify in the IIR)
L_AgriOther	3Da1	Inorganic N-fertilizers (includes also urea application)
	3Da2a	Animal manure applied to soils
	3Da2b	Sewage sludge applied to soils
	3Da2c	Other organic fertilisers applied to soils (including compost)
	3Da3	Urine and dung deposited by grazing animals
	3Da4	Crop residues applied to soils
	3Db	Indirect emissions from managed soils
	3Dc	Farm-level agricultural operations including storage, handling and transport of agricultural products
	3Dd	Off-farm storage, handling and transport of bulk agricultural products
	3De	Cultivated crops
	3Df	Use of pesticides
	3F	Field burning of agricultural residues
	3I	Agriculture other (please specify in the IIR)
M_Other	6A	Other (included in national total for entire territory) (please specify in the IIR)

Table A.3. *Annual* ***lead*** *emissions from the OSPAR Contracting Parties. Units: t/y.*

Pb, t	1990	1991	1992	1993	1994	1995	1996	1997	1998	1999	2000	2001	2002	2003	2004
Belgium	264	248	259	221	175	207	219	238	163	177	107	83.5	83.4	80.5	89.2
Denmark	130	109	100	58.8	26.4	26.0	24.9	23.0	25.0	31.6	19.6	18.7	18.1	19.1	21.1
Finland	321	237	165	105	73.9	72.7	49.2	31.8	37.2	34.8	30.6	30.4	30.7	24.9	26.5
France	4294	2887	2107	1852	1650	1476	1309	1159	1041	809	283	250	246	196	183
Germany	1919	1476	1150	967	776	716	578	451	403	393	401	362	341	310	298
Iceland	0.31	0.29	0.33	0.75	0.74	0.83	1.00	1.03	1.09	1.32	1.19	1.30	1.16	1.34	1.38
Ireland	158	142	150	130	113	98.4	82.8	87.1	59.1	34.8	14.2	12.7	11.7	11.7	11.9
Luxembourg	18.8	17.9	16.4	18.0	15.1	8.96	8.62	5.53	1.80	1.47	1.09	1.06	1.01	1.66	1.82
Netherlands	89.7	84.1	81.7	79.3	76.8	75.0	62.4	52.3	42.3	34	26.6	30.9	34.9	31.4	32.9
Norway	189	146	130	90.3	27.7	25.0	13.4	13.0	13.6	12.9	11.2	9.9	10.5	10.8	11.0
Portugal	575	631	708	751	775	796	327	335	347	351	43.7	41.8	42.1	42.0	42.8
Spain	2587	1711	1124	1017	1001	856	819	753	689	621	476	260	133	133	132
Sweden	354	309	288	138	46.5	32.2	27.9	28.2	27.2	25.1	21.9	20.3	17.4	17.4	16.5
Switzerland	379	350	320	263	232	169	145	131	89.3	52.9	30.8	28.1	24.9	22.1	21.6
United Kingdom	2921	2667	2446	2171	1872	1563	1327	1173	869	520	189	181	175	172	164
OSPAR	**14200**	**11015**	**9046**	**7863**	**6861**	**6123**	**4995**	**4482**	**3810**	**3101**	**1657**	**1331**	**1171**	**1073**	**1054**
Other	29072	25738	22347	21417	19297	17478	16101	14947	13878	12714	11192	9489	7863	7609	4290
EMEP	43272	36754	31393	29279	26158	23601	21097	19429	17688	15815	12848	10820	9033	8682	5344

Table A.3. ***(continued)*** *Annual* ***lead*** *emissions from the OSPAR Contracting Parties. Units: t/y.*

Pb, t	2005	2006	2007	2008	2009	2010	2011	2012	2013	2014	2015	2016	2017	2018	2019	2020
Belgium	73.8	72.3	61.9	72.1	31.0	40.0	29.6	28.9	25.6	23.0	29.4	27.3	25.5	13.6	14.6	11.8
Denmark	17.4	16.3	13.9	14.0	13.1	12.8	12.5	12.1	12.2	11.6	11.9	12.1	12.1	12.5	12.0	11.5
Finland	21.4	24.9	21.8	19.8	16.8	20.4	19.2	16.3	16.0	16.6	14.7	15.7	15.6	15.4	13.2	11.6
France	179	171	167	152	126	138	127	128	124	120	114	114	115	114	84.8	72.4
Germany	269	257	241	214	188	212	207	202	200	201	209	203	211	207	161	142.6
Iceland	1.41	2.23	2.44	1.78	1.41	1.45	1.29	1.25	0.55	0.58	0.64	0.68	0.66	0.77	0.56	0.6
Ireland	8.05	7.60	7.47	7.39	6.60	6.24	5.76	5.67	5.74	5.47	5.51	5.36	5.06	5.10	4.80	4.1
Luxembourg	1.39	1.30	1.24	1.37	1.04	1.00	1.51	1.67	1.12	1.24	1.33	1.27	1.34	1.20	1.46	1.2
Netherlands	29.1	29.3	34.9	29.6	30.6	36.8	21.6	15.2	13.0	8.20	7.85	8.12	7.75	5.04	5.16	5.9
Norway	9.8	9.25	8.22	7.32	5.22	6.04	6.23	5.59	5.76	5.59	6.35	5.79	5.82	5.83	6.09	5.3
Portugal	42.5	43.4	44.0	43.7	40.4	40.5	40.6	40.5	40.0	40.4	39.9	39.5	40.1	43.0	25.3	23.1
Spain	130	131	132	126	112	117	96.4	88.0	94.6	95.4	94.2	90.0	86.6	89.9	98.5	82.2
Sweden	14.3	13.9	14.7	12.9	12.1	12.7	11.4	11.2	10.7	11.2	10.3	11.1	11.1	9.79	8.09	6.9
Switzerland	20.0	18.7	19.0	18.3	17.2	16.6	16.3	16.5	16.5	14.8	15.0	14.8	15.0	15.2	14.9	13.9
United Kingdom	155	136	124	115	101	102	101	105	98.9	107	106	96.5	95.6	92.8	92.6	90.2
OSPAR	**973**	**933**	**893**	**836**	**702**	**764**	**698**	**677**	**665**	**662**	**665**	**645**	**648**	**631**	**543**	**483**
Other	3913	3779	3706	3529	3081	3063	2838	2825	2678	2628	2564	2542	2577	2577	2394	2243
EMEP	4886	4712	4600	4365	3783	3826	3536	3502	3343	3290	3230	3188	3225	3208	2937	2726

Table A.4. *Annual* ***cadmium*** *emissions from the OSPAR Contracting Parties. Units: t/y.*

	1990	1991	1992	1993	1994	1995	1996	1997	1998	1999	2000	2001	2002	2003	2004	2005	2006
Belgium	6.25	6.03	6.78	5.60	4.09	5.10	4.18	4.35	2.41	2.36	2.78	2.49	2.35	2.45	2.87	2.15	2.32
Denmark	1.21	1.24	1.08	0.99	0.84	0.71	0.73	0.69	0.66	0.65	0.64	0.69	0.66	0.69	0.69	0.70	0.67
Finland	6.67	3.80	3.31	3.37	2.70	2.13	1.91	1.53	1.69	1.53	1.41	1.74	1.37	1.32	1.61	1.46	1.42
France	20.4	20.4	19.8	18.9	18.8	17.9	17.4	16.4	15.5	14.2	14.2	13.0	12.3	9.04	6.58	5.89	4.69
Germany	30.4	26.9	24.2	22.9	22.5	20.4	20.9	20.6	19.9	19.9	18.8	17.8	17.2	15.7	14.5	12.9	13.7
Iceland	0.01	0.01	0.01	0.02	0.02	0.03	0.03	0.03	0.03	0.03	0.03	0.03	0.03	0.03	0.03	0.03	0.05
Ireland	0.59	0.58	0.54	0.58	0.54	0.57	0.59	0.59	0.62	0.58	0.59	0.48	0.36	0.33	0.34	0.37	0.36
Luxembourg	0.09	0.09	0.09	0.09	0.09	0.07	0.08	0.07	0.06	0.06	0.06	0.06	0.07	0.07	0.14	0.08	0.08
Netherlands	2.08	1.78	1.60	1.42	1.23	1.06	0.94	1.03	1.12	0.93	0.92	1.60	2.17	2.32	1.73	1.67	1.93
Norway	1.66	1.53	1.40	1.54	1.52	1.30	1.40	1.34	1.40	1.32	1.05	0.97	0.94	0.90	0.83	0.78	0.82
Portugal	2.44	2.44	2.48	2.36	2.44	2.58	2.67	2.84	2.88	2.82	2.77	2.68	2.62	2.47	2.51	2.51	2.45
Spain	27.7	26.2	23.3	20.7	20.5	20.9	22.0	21.3	22.0	21.2	14.9	12.3	12.8	11.5	10.8	9.77	8.15
Sweden	2.31	1.74	1.37	1.08	0.77	0.75	0.71	0.71	0.63	0.54	0.52	0.60	0.52	0.52	0.54	0.54	0.56
Switzerland	3.68	3.47	3.30	3.09	2.85	2.49	2.37	2.19	1.92	1.65	1.47	1.32	1.14	1.03	1.03	1.04	1.05
United Kingdom	25.6	25.0	23.8	13.1	12.6	11.0	9.55	8.65	6.87	6.43	5.66	5.35	5.17	4.48	4.43	4.48	4.47
OSPAR	**131**	**121**	**113**	**95.8**	**91.5**	**86.9**	**85.4**	**82.4**	**77.7**	**74.2**	**65.8**	**61.1**	**59.7**	**52.9**	**48.6**	**44.4**	**42.7**
Other	277	252	244	223	216	213	200	195	187	181	175	172	161	197	171	180	178
EMEP	408	373	357	319	308	300	286	277	264	255	241	233	221	250	220	224	221

Table A.4. ***(continued)*** *Annual* ***cadmium*** *emissions from the OSPAR Contracting Parties. Units: t/y.*

	2007	2008	2009	2010	2011	2012	2013	2014	2015	2016	2017	2018	2019	2020
Belgium	2.12	2.42	1.55	1.96	1.67	1.47	1.47	1.25	1.63	2.58	1.35	1.20	1.19	1.03
Denmark	0.75	0.73	0.70	0.72	0.68	0.66	0.68	0.67	0.74	0.76	0.78	0.80	0.71	0.67
Finland	1.26	1.21	1.16	1.29	1.22	1.17	1.08	0.92	0.89	0.94	0.96	0.88	0.79	0.70
France	4.33	4.37	3.31	3.34	3.10	2.95	3.03	3.18	2.94	3.39	3.11	2.64	2.62	2.55
Germany	13.2	12.1	10.9	13.3	13.3	13.0	13.0	12.7	13.1	12.8	13.1	12.7	10.8	10.75
Iceland	0.05	0.04	0.03	0.03	0.03	0.02	0.01	0.01	0.01	0.01	0.00	0.01	0.01	0.00
Ireland	0.34	0.33	0.31	0.30	0.28	0.29	0.28	0.30	0.31	0.30	0.30	0.28	0.25	0.24
Luxembourg	0.08	0.41	0.13	0.07	0.07	0.11	0.06	0.07	0.08	0.08	0.07	0.07	0.06	0.06
Netherlands	1.70	1.87	1.78	2.51	1.10	0.79	0.60	0.54	0.53	0.54	0.63	2.32	2.64	2.02
Norway	0.76	0.74	0.59	0.73	0.69	0.59	0.54	0.46	0.51	0.47	0.49	0.51	0.50	0.47
Portugal	2.36	2.33	2.17	2.14	2.21	2.12	2.04	2.03	2.07	1.99	2.04	2.04	1.83	1.80
Spain	6.78	6.17	5.30	5.31	5.92	5.01	5.03	4.79	5.02	4.75	4.86	4.90	7.36	5.60
Sweden	0.57	0.52	0.54	0.54	0.52	0.53	0.50	0.52	0.48	0.48	0.52	0.48	0.49	0.49
Switzerland	1.05	1.11	1.11	1.15	1.08	1.16	1.22	1.09	1.12	1.17	1.18	1.16	0.69	0.59
United Kingdom	3.68	3.59	3.43	3.77	3.93	3.53	3.66	4.10	3.92	3.68	3.88	4.05	5.59	4.54
OSPAR	**39.1**	**38.0**	**33.0**	**37.2**	**35.8**	**33.4**	**33.2**	**32.7**	**33.3**	**34.0**	**33.2**	**34.0**	**35.6**	**31.5**
Other	180	177.0	166.2	160.6	158.4	155.8	150.6	148.0	143.5	142.4	142.5	140.6	99.1	96.4
EMEP	219	214.9	199.2	197.8	194.3	189.1	183.8	180.6	176.9	176.4	175.7	174.7	134.7	127.9

Table A.5. *Annual* ***mercury*** *emissions from the OSPAR Contracting Parties. Units: t/y.*

	1990	1991	1992	1993	1994	1995	1996	1997	1998	1999	2000	2001	2002	2003	2004	2005	2006
Belgium	6.08	5.81	5.73	3.72	4.14	3.35	3.29	3.76	2.69	3.06	3.21	2.84	3.86	3.66	3.56	2.16	2.07
Denmark	3.16	3.28	3.00	2.93	2.54	2.32	2.46	1.98	1.68	1.48	1.00	0.87	0.84	0.87	0.73	0.69	0.61
Finland	1.08	0.93	0.89	0.76	0.80	0.80	0.86	0.80	0.69	0.63	0.60	0.68	0.67	0.82	0.75	0.89	1.03
France	25.6	26.1	24.8	22.8	22.3	21.1	20.1	15.9	14.3	12.8	12.3	10.9	9.93	7.29	6.94	7.25	7.07
Germany	35.4	29.9	25.3	22.6	21.3	20.2	19.7	19.4	19.0	18.2	18.2	17.6	16.6	15.9	15.2	14.0	13.4
Iceland	0.14	0.14	0.14	0.13	0.12	0.11	0.11	0.11	0.09	0.08	0.08	0.08	0.07	0.07	0.05	0.04	0.05
Ireland	0.83	0.81	0.73	0.74	0.68	0.67	0.70	0.66	0.46	0.41	0.44	0.44	0.42	0.43	0.43	0.45	0.43
Luxembourg	0.41	0.40	0.38	0.39	0.35	0.23	0.17	0.13	0.09	0.22	0.27	0.29	0.15	0.21	0.16	0.20	0.30
Netherlands	3.52	2.91	2.49	2.07	1.65	1.42	1.21	1.01	0.80	0.90	1.02	0.84	0.73	0.68	0.85	0.87	0.81
Norway	1.46	1.36	1.20	0.88	1.01	0.80	0.82	0.83	0.78	0.82	0.64	0.59	0.57	0.70	0.57	0.56	0.51
Portugal	2.20	2.24	2.26	2.21	2.32	2.46	2.55	2.82	2.63	2.58	2.37	2.08	2.02	1.91	1.96	1.84	1.83
Spain	10.6	10.8	11.6	10.2	10.4	12.8	10.6	9.80	10.3	10.9	8.83	7.82	8.72	7.42	7.31	7.31	6.49
Sweden	1.54	1.23	1.16	1.02	1.04	0.97	1.03	0.84	0.85	0.85	0.73	0.57	0.61	0.69	0.70	0.65	0.50
Switzerland	6.37	5.85	5.54	5.15	4.72	3.89	3.61	3.35	2.55	2.29	1.77	1.44	1.05	0.72	0.74	0.76	0.79
United Kingdom	38.2	38.4	36.6	22.1	20.8	20.2	14.9	11.6	10.7	8.36	8.33	8.17	7.24	7.58	6.81	7.51	7.55
OSPAR	**137**	**130**	**122**	**97.7**	**94.2**	**91.3**	**82.1**	**73.0**	**67.6**	**63.6**	**59.8**	**55.2**	**53.5**	**49.0**	**46.8**	**45.1**	**43.4**
Other	180	172	162	159	155	154	152	149	146	142	143	141	122	151	126	128	138
EMEP	317	302	284	256	249	245	234	222	213	206	202	197	176	200	173	173	182

Table A.5. ***(continued)*** *Annual* ***mercury*** *emissions from the OSPAR Contracting Parties. Units: t/y.*

	2007	2008	2009	2010	2011	2012	2013	2014	2015	2016	2017	2018	2019	2020
Belgium	3.19	3.61	1.74	1.74	1.68	1.30	1.39	1.52	1.08	1.38	1.05	1.37	1.03	0.99
Denmark	0.59	0.59	0.45	0.43	0.38	0.29	0.33	0.32	0.28	0.33	0.28	0.27	0.23	0.24
Finland	0.87	0.82	0.76	0.89	0.75	0.74	0.76	0.71	0.62	0.59	0.58	0.68	0.59	0.54
France	5.41	4.77	4.47	4.78	4.92	4.38	4.30	4.62	4.00	3.48	3.30	3.19	3.00	2.38
Germany	12.6	11.1	10.3	11.1	10.5	10.2	9.78	9.63	9.44	8.63	8.55	8.25	7.21	6.29
Iceland	0.06	0.05	0.04	0.04	0.03	0.03	0.01	0.01	0.02	0.02	0.02	0.01	0.01	0.01
Ireland	0.42	0.41	0.38	0.36	0.34	0.36	0.35	0.34	0.35	0.35	0.34	0.30	0.33	0.27
Luxembourg	0.27	0.16	0.06	0.07	0.06	0.09	0.16	0.07	0.08	0.12	0.06	0.06	0.10	0.08
Netherlands	0.75	0.64	0.68	0.63	0.73	0.63	0.61	0.57	0.58	0.62	0.50	0.51	0.59	0.50
Norway	0.47	0.43	0.35	0.38	0.34	0.31	0.31	0.27	0.24	0.26	0.24	0.22	0.22	0.21
Portugal	1.81	1.74	1.70	1.67	1.51	1.46	1.40	1.38	1.44	1.41	1.48	1.43	1.27	1.22
Spain	5.81	4.95	4.29	4.19	4.29	4.59	4.00	4.15	4.34	4.37	4.30	4.06	3.08	2.68
Sweden	0.55	0.49	0.53	0.51	0.49	0.45	0.48	0.42	0.40	0.40	0.40	0.40	0.40	0.37
Switzerland	0.79	0.79	0.75	0.77	0.74	0.72	0.71	0.69	0.69	0.69	0.67	0.67	0.68	0.64
United Kingdom	7.08	6.94	6.41	6.47	5.95	5.74	6.03	5.36	4.76	4.04	4.03	3.95	4.01	3.37
OSPAR	**40.7**	**37.5**	**32.9**	**34.0**	**32.7**	**31.3**	**30.6**	**30.1**	**28.3**	**26.7**	**25.8**	**25.4**	**22.7**	**19.8**
Other	129	126	116	117	118	117	114	111	108	107	108	113	115	120.6
EMEP	170	164	149	151	150	148	144	141	136	133	134	139	138	140.4

Table A.6. *Annual **lead** emissions from GNFR sectors in the OSPAR Contracting Parties in 2020. Units: t/y.*

GNFR	BE	DK	FI	FR	DE	IS	IE
A_PublicPower	0.333	0.321	1.684	3.832	5.872	9.8E-05	0.340
B_Industry	7.348	2.171	7.337	26.260	70.393	0.001	0.378
C_OtherStatComb	0.855	0.972	1.691	9.380	21.903	1.8E-04	1.810
D_Fugitive	0.142	4.4E-04	0.027	0.258	NA	MR	MR
E_Solvents	0.620	0.034	0.365	2.075	0.001	0.387	0.008
F_RoadTransport	2.204	5.155	0.469	24.962	44.052	0.086	1.197
G_Shipping	0.015	0.019	0.009	0.054	0.039	0.001	0.013
H_Aviation	0.066	0.598	0.046	2.085	0.244	NA	0.379
I_Offroad	0.189	0.037	0.004	0.003	0.086	0.061	0.002
J_Waste	0.015	2.165	0.001	3.210	0.053	0.038	0.012
L_AgriOther	MR	0.006	0.002	0.250	MR	MR	MR
M_Other	NO	NO	NO	NO	NA	NO	NO
Total	**11.8**	**11.5**	**11.6**	**72.4**	**142.6**	**0.6**	**4.1**

Table A.6 (continued). *Annual **lead** emissions from GNFR sectors in the OSPAR Contracting Parties in 2020. Units: t/y.*

GNFR	LU	NL	NO	PT	ES	SE	CH	GB
A_PublicPower	0.171	0.160	0.120	0.411	0.546	1.913	1.661	2.139
B_Industry	0.300	3.596	1.711	12.843	42.645	3.703	1.094	39.371
C_OtherStatComb	0.115	0.078	0.767	0.948	3.454	0.660	0.594	3.320
D_Fugitive	MR	0.000	0.000	0.255	0.001	0.001	6.5E-06	0.782
E_Solvents	0.005	0.107	0.000	0.287	0.002	1.7E-04	0.336	4.288
F_RoadTransport	0.524	0.896	1.873	7.402	28.471	0.439	2.046	33.197
G_Shipping	7.9E-08	8.1E-05	0.081	0.011	0.075	0.014	0.012	0.167
H_Aviation	0.124	0.735	0.447	0.858	0.268	0.129	0.724	0.280
I_Offroad	5.1E-05	0.239	0.110	0.009	0.302	0.011	0.027	6.410
J_Waste	3.8E-04	0.046	0.198	0.051	6.398	0.018	1.741	0.292
L_AgriOther	MR	MR	0.005	0.031	0.033	MR	MR	MR
M_Other	NA	NE	NE	NO	NA	NO	5.646	NA
Total	**1.2**	**5.9**	**5.3**	**23.1**	**82.2**	**6.9**	**13.9**	**90.2**

NA – not applicable, the process or activity exists but do not result in emissions of a specific pollutant.

NO – not occurring, an activity or process does not occur within a country.

NE – not estimated, an activity and/or emissions by sources of pollutants which have not been estimated but for which a corresponding activity may occur within a country.

MR – multiple reasons

Table A.7. *Annual **cadmium** emissions from GNFR sectors in the OSPAR Contracting Parties in 2020. Units: t/y.*

GNFR	BE	DK	FI	FR	DE	IS	IE
A_PublicPower	0.129	0.026	0.116	0.192	0.626	3.3E-05	0.039
B_Industry	0.402	0.076	0.283	1.342	8.283	0.001	0.100
C_OtherStatComb	0.298	0.458	0.261	0.139	0.730	3.5E-06	0.038
D_Fugitive	0.035	0.001	0.001	0.052	NA	MR	MR
E_Solvents	0.133	0.003	0.012	0.328	0.850	0.001	0.049
F_RoadTransport	0.012	0.045	0.002	0.117	0.204	0.001	0.006
G_Shipping	0.001	0.002	0.001	0.017	0.004	7.8E-05	0.001
H_Aviation	2.5E-06	1.1E-05	NA	NE	1.2E-07	NA	1.2E-05
I_Offroad	0.010	0.006	0.008	0.001	0.011	0.002	0.002
J_Waste	0.009	0.006	0.001	0.210	0.037	2.8E-04	0.001
L_AgriOther	MR	0.050	0.017	0.154	MR	MR	MR
M_Other	NO	NO	NO	NO	NA	NO	NO
Total	**1.029**	**0.673**	**0.700**	**2.552**	**10.745**	**0.005**	**0.236**

Table A.7 (continued). *Annual **cadmium** emissions from GNFR sectors in the OSPAR Contracting Parties in 2020. Units: t/y.*

GNFR	LU	NL	NO	PT	ES	SE	CH	GB
A_PublicPower	0.011	0.044	0.054	0.048	0.212	0.144	0.157	0.143
B_Industry	0.027	1.678	0.116	0.881	2.725	0.192	0.052	2.055
C_OtherStatComb	0.010	0.051	0.183	0.437	1.102	0.130	0.038	0.459
D_Fugitive	MR	1.3E-05	0.001	0.054	2.3E-04	3.7E-04	8.8E-06	0.010
E_Solvents	0.003	0.091	0.002	0.146	0.317	0.001	0.074	1.564
F_RoadTransport	0.005	0.130	0.057	0.010	0.244	0.003	0.084	0.156
G_Shipping	0.000	1.4E-05	0.008	0.001	0.007	0.001	0.003	0.014
H_Aviation	MR	4.3E-05	0.001	1.7E-05	1.2E-05	NE	NA	0.005
I_Offroad	0.000	8.0E-05	0.012	0.001	0.038	0.013	0.032	0.085
J_Waste	0.001	0.022	0.002	0.006	0.699	0.006	0.009	0.046
L_AgriOther	MR	MR	0.038	0.213	0.260	MR	MR	MR
M_Other	NA	NE	NE	NO	NA	NO	0.141	NA
Total	**0.057**	**2.017**	**0.473**	**1.798**	**5.604**	**0.489**	**0.591**	**4.536**

NA – not applicable, the process or activity exists but do not result in emissions of a specific pollutant.

NO – not occurring, an activity or process does not occur within a country.

NE – not estimated, an activity and/or emissions by sources of pollutants which have not been estimated but for which a corresponding activity may occur within a country.

MR – multiple reasons

Table A.8. *Annual **mercury** emissions from GNFR sectors in the OSPAR Contracting Parties in 2020. Units: t/y.*

GNFR	BE	DK	FI	FR	DE	IS	IE
A_PublicPower	0.176	0.107	0.105	0.406	3.137	3.3E-05	0.058
B_Industry	0.610	0.061	0.340	1.244	2.415	7.2E-05	0.073
C_OtherStatComb	0.084	0.026	0.042	0.119	0.336	1.7E-05	0.079
D_Fugitive	0.025	3.1E-04	1.0E-05	0.013	0.022	MR	MR
E_Solvents	0.002	4.7E-04	2.7E-05	0.110	NA	3.1E-05	5.4E-07
F_RoadTransport	0.043	0.022	0.023	0.207	0.299	0.002	0.019
G_Shipping	0.005	0.004	0.002	0.003	0.007	2.4E-04	0.003
H_Aviation	1.9E-04	8.8E-06	NA	NE	5.1E-06	NA	2.2E-04
I_Offroad	0.002	0.006	0.001	0.010	0.021	0.005	0.001
J_Waste	0.047	0.002	0.022	0.242	0.052	0.008	0.034
L_AgriOther	MR	0.008	0.003	0.023	MR	MR	MR
M_Other	NO	NO	NO	NO	NA	NO	NO
Total	**0.994**	**0.237**	**0.538**	**2.377**	**6.290**	**0.015**	**0.267**

Table A.8 (continued). *Annual **mercury** emissions from GNFR sectors in the OSPAR Contracting Parties in 2020. Units: t/y.*

GNFR	LU	NL	NO	PT	ES	SE	CH	GB
A_PublicPower	0.010	0.080	0.018	0.082	0.387	0.133	0.301	0.712
B_Industry	0.053	0.265	0.090	0.783	1.529	0.145	0.141	1.376
C_OtherStatComb	0.003	0.036	0.014	0.032	0.137	0.022	0.076	0.202
D_Fugitive	MR	0.001	3.3E-04	0.141	2.7E-04	5.7E-05	1.5E-06	0.007
E_Solvents	3.5E-07	0.002	0.005	0.058	0.105	3.8E-04	1.0E-04	3.1E-04
F_RoadTransport	0.009	0.087	0.014	0.025	0.129	0.037	0.032	0.177
G_Shipping	7.7E-07	0.001	0.040	0.001	0.013	2.1E-04	2.0E-04	0.035
H_Aviation	MR	NE	0.002	0.001	0.001	NE	NA	3.9E-05
I_Offroad	3.8E-04	0.006	0.017	0.002	0.010	1.3E-06	0.002	0.053
J_Waste	0.001	0.018	0.003	0.057	0.331	0.034	0.029	0.803
L_AgriOther	MR	MR	0.006	0.035	0.041	MR	MR	MR
M_Other	NA	NE	NE	NO	NA	NO	0.063	NA
Total	**0.076**	**0.495**	**0.211**	**1.217**	**2.682**	**0.371**	**0.643**	**3.366**

NA – not applicable, the process or activity exists but do not result in emissions of a specific pollutant.

NO – not occurring, an activity or process does not occur within a country.

NE – not estimated, an activity and/or emissions by sources of pollutants which have not been estimated but for which a corresponding activity may occur within a country.

MR – multiple reasons

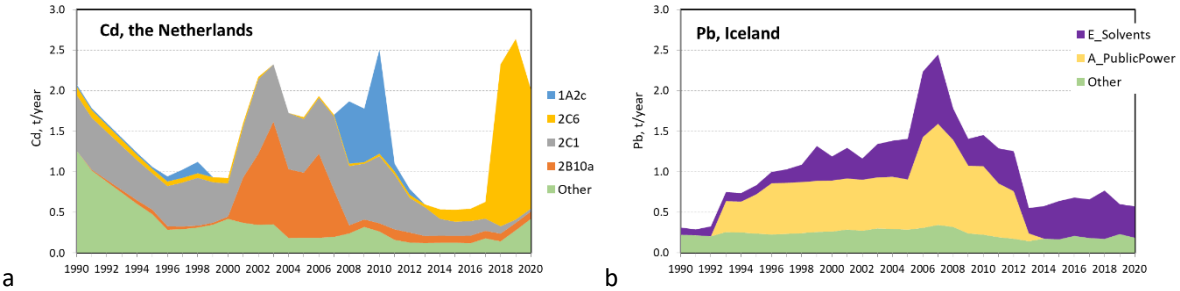

a b

Fig. A.1. *Time series of main Cd NFR emission sectors in the Netherlands (a) and Pb GNFR emission sectors in Iceland (b) form 1990 to 2020 used in the report. 1A2C - Stationary combustion in manufacturing industries and construction: Chemicals; 2B10a - Chemical industry: Other; 2C1 - Iron and steel production; 2C6 - Zinc production.*

Table A.9. *Main NFR emission sectors in the OSPAR Contracting Parties in 2020.*

Metal	GNFR sector	GNFR emission, t/y	% of OSPAR total	NFR code	NFR sector	NFR OSPAR total t/y	% of GNFR sector
Pb	B_Industry	219.2	45	1A2a	Stationary combustion in manufacturing industries and construction: Iron and steel	21.8	10
				2A3	Glass production	15.8	7
				2C1	Iron and steel production	106.6	49
				1A2gviii	Stationary combustion in manufacturing industries and construction: Other	13.0	6
	C_OtherStatComb	46.5	10	1A4ai	Commercial/Institutional: Stationary	20.7	44
				1A4bi	Residential: Stationary	23.2	50
	F_RoadTransport	153.0	32	1A3bi	Road transport: Passenger cars	24.9	16
				1A3bvi	Road transport: Automobile tyre and brake wear	120.8	79
Cd	B_Industry	18.2	58	2C1	Iron and steel production	3.2	18
				2C6	Zinc production	1.7	9
					Stationary combustion in manufacturing industries and construction: Other	2.1	12
				2C7a	Copper production	5.7	31
	C_OtherStatComb	4.3	14	1A4ai	Commercial/Institutional: Stationary	0.4	8
				1A4bi	Residential: Stationary	3.8	87
	E_Solvents	3.6	11	2G	Other product use	3.5	99
Hg	A_PublicPower	5.7	29	1A1a	Public electricity and heat production	5.7	100
	B_Industry	9.1	46	1A2d	Stationary combustion in manufacturing industries and construction: Pulp, Paper and Print	0.7	8
				1A2f	Stationary combustion in manufacturing industries and construction: Non-metallic minerals	1.3	14
				1A2gviii	Stationary combustion in manufacturing industries and construction: Other	0.8	9
				2A1	Cement production	0.8	9
				2C1	Iron and steel production	2.5	28
	J_Waste	1.7	9	5A	Biological treatment of waste - Solid waste disposal on land	0.4	21
				5C1biv	Sewage sludge incineration	0.2	10

	5C1bv	Cremation	0.9	56

Table A.10. *Annual modelled* ***lead*** *total deposition to the main regions of the OSPAR maritime area. Units: t/y.*

OSPAR region	I. Arctic Waters	II. Greater North Sea	III. Celtic Seas	IV. Bay of Biscay	V. Wider Atlantic
Area, km²	5480370	748586	381919	538114	6329170
1990	1487	1432	312	439	2333
1991	1479	1304	370	462	2243
1992	1516	1244	276	389	2660
1993	1353	1079	377	457	2447
1994	1363	1078	313	248	2032
1995	1322	985	302	361	2315
1996	1173	814	319	298	1823
1997	1068	857	280	272	2326
1998	1045	797	279	313	2280
1999	1051	676	159	290	1681
2000	1007	591	162	205	2046
2001	859	354	92.3	200	1488
2002	860	373	147	203	1928
2003	886	316	132	189	1504
2004	810	323	91.5	195	1461
2005	798	290	84.8	106	1236
2006	762	290	96.1	152	1569
2007	699	237	77.8	180	1373
2008	830	348	105	128	1614
2009	677	229	76.2	105	1287
2010	602	192	57.8	121	1089
2011	827	238	78.0	107	1249
2012	609	210	83.7	86.1	1037
2013	630	209	83.8	94.7	1334
2014	660	281	93.9	111	1316
2015	761	214	94.3	95.6	1280
2016	606	174	76.6	83.8	1222
2017	631	188	70.8	84.6	1079
2018	659	187	76.0	86.2	1225
2019	633	189	79.5	77.6	1197
2020	763	220	100.7	99.5	1257

Table A.11. *Annual modelled* ***cadmium*** *total deposition to the main regions of the OSPAR maritime area. Units: t/y.*

OSPAR region	I. Arctic Waters	II. Greater North Sea	III. Celtic Seas	IV. Bay of Biscay	V. Wider Atlantic
Area, km²	5480370	748586	381919	538114	6329170
1990	38.6	40.7	6.5	8.6	58.6
1991	38.3	34.4	7.5	8.9	57.9
1992	40.6	38.8	5.7	8.0	63.3
1993	37.5	30.9	7.5	9.0	60.1
1994	37.6	33.5	7.4	5.8	55.8
1995	36.4	30.0	6.7	7.4	55.3
1996	33.2	23.7	8.4	8.1	52.8
1997	30.5	24.0	6.6	6.6	59.8
1998	30.3	23.2	5.9	7.3	56.4
1999	30.6	23.7	4.6	7.0	49.2
2000	29.5	23.0	4.7	5.8	53.9
2001	27.5	16.3	3.7	6.4	47.8
2002	28.6	19.4	5.6	7.2	58.7
2003	29.6	15.5	4.9	5.9	49.2
2004	29.4	17.0	3.6	5.9	44.0
2005	28.0	15.7	3.3	3.7	40.4
2006	28.3	15.7	3.6	5.2	50.0
2007	26.4	12.5	3.0	5.2	44.7
2008	28.8	16.5	3.9	4.2	48.3
2009	24.7	11.4	3.1	3.6	43.0
2010	23.3	9.3	2.3	4.2	37.9
2011	30.0	13.1	3.1	3.6	43.1
2012	23.5	9.0	2.9	2.9	35.7
2013	24.1	9.5	3.1	3.5	47.2
2014	24.8	11.8	3.3	3.7	45.3
2015	28.9	10.0	3.4	3.2	44.4
2016	23.6	8.2	2.9	3.0	43.2
2017	24.8	8.7	2.7	3.0	38.7
2018	25.9	9.5	3.1	3.3	44.2
2019	21.8	7.0	2.8	2.7	39.6
2020	27.8	7.7	3.5	3.2	42.2

Table A.12. *Annual modelled* ***mercury*** *total deposition to the main regions of the OSPAR maritime area. Units: t/y.*

OSPAR region	I. Arctic Waters	II. Greater North Sea	III. Celtic Seas	IV. Bay of Biscay and Iberian Coast	V. Wider Atlantic
Area, km²	5480370	748586	381919	538114	6329170
1990	59.64	9.68	3.38	3.11	50.70
1991	60.27	9.18	3.83	3.61	50.54
1992	56.77	9.67	3.54	3.30	47.38
1993	59.65	7.73	3.60	3.58	47.06
1994	55.26	8.30	3.63	3.18	46.30
1995	55.57	7.43	3.21	3.58	46.08
1996	53.00	6.92	3.27	3.32	43.36
1997	54.65	6.90	2.92	3.13	45.81
1998	50.05	7.48	3.32	3.07	44.75
1999	52.38	6.58	2.79	3.31	41.98
2000	56.34	7.26	2.74	3.48	42.61
2001	52.67	6.78	2.62	3.37	43.99
2002	49.21	6.52	3.06	3.47	45.59
2003	52.61	6.08	2.73	3.24	45.76
2004	48.68	5.86	2.54	3.02	40.69
2005	54.03	6.24	2.70	2.65	43.70
2006	50.90	6.32	2.77	3.25	45.94
2007	54.47	5.98	2.51	2.94	43.84
2008	52.48	5.86	2.67	2.97	42.98
2009	54.08	5.83	2.71	2.81	43.32
2010	47.88	5.53	2.36	3.13	41.47
2011	50.30	5.85	2.45	2.52	42.26
2012	46.91	6.01	2.85	2.93	39.38
2013	51.54	5.33	2.41	2.95	43.80
2014	47.40	5.92	2.44	3.04	40.29
2015	48.76	5.59	2.79	2.63	43.34
2016	43.70	4.89	2.57	2.71	43.01
2017	47.53	5.63	2.42	2.27	39.07
2018	46.17	5.07	2.20	2.46	39.47
2019	40.74	5.38	2.47	2.24	39.20
2020	48.51	4.92	2.56	2.59	37.35

Annex B.
Modelled and observed air concentrations and wet deposition at the CAMP stations

Table B.1. *Annual mean modelled and observed Pb air concentrations, ng/m^3, and mean relative bias at CAMP stations in 2020.*

Code	Name	Longit	Latid	Observed	Modelled	Bias, %
BE14	Koksijde	2.66	51.12	3.05	5.70	87
DE1	Westerland	8.31	54.93	1.16	2.05	77
DK8	Anholt	11.52	56.72	0.79	1.57	99
DK10	Nord	-16.67	81.6	0.14	0.04	-75
DK12	Riscoe	12.09	55.69	1.10	3.18	189
ES8	Niembro	-4.85	43.44	1.70	2.05	21
GB13	Yarner Wood	-3.71	50.6	1.53	1.94	27
GB17	Heigham Holmes	1.62	52.72	3.04	3.51	16
GB48	Auchencorth Moss	-3.24	55.79	0.80	1.31	64
IS91	Vestmannaeyjar	-20.29	63.4	0.07	0.65	781
NO2	Birkenes II	8.25	58.39	0.49	0.63	27
NO42	Zeppelin	11.89	78.91	0.26	0.14	-44
NO90	Alomar	16.01	69.28	0.10	0.43	349
SE14	Råö	11.91	57.39	0.66	1.21	82

Table B.2. *Annual sums of modelled and observed Pb wet deposition fluxes, g/km^2/year, and mean relative bias at CAMP stations in 2020.*

Code	Name	Longit	Latid	Observed	Modelled	Bias, %
BE14	Koksijde	2.66	51.12	281	312	11
DE1	Westerland	8.31	54.93	182	414	128
DK5	Keldsnor	10.74	54.75	418	134	-68
DK8	Anholt	11.52	56.72	344	196	-43
DK12	Riscoe	12.09	55.69	296	230	-22
DK22	Sepstrup Sande	9.42	56.08	420	229	-45
DK31	Ulborg	8.43	56.29	403	346	-14
ES8	Niembro	-4.85	43.44	1717	151	-91
FR90	Porspoder	-4.75	48.52	328	305	-7
GB6	Lough Navar	-7.87	54.44	53	139	163
GB13	Yarner Wood	-3.71	50.6	33	109	229
GB17	Heigham Holmes	1.62	52.72	79	53	-32
GB48	Auchencorth Moss	-3.24	55.79	29	91	210
NL91	De Zilk	4.5	52.3	287	265	-8
NO1	Birkenes	8.25	58.38	1063	422	-60
NO39	Kårvatn	8.88	62.78	242	141	-42
SE14	Råö	11.91	57.39	186	321	72

Table B.3. *Annual mean modelled and observed Cd air concentrations, ng/m^3, and mean relative bias at CAMP stations in 2020.*

Code	Name	Longit	Latid	Observed	Modelled	Bias, %
BE14	Koksijde	2.66	51.12	0.081	0.233	187
DE1	Westerland	8.31	54.93	0.042	0.086	108
DK8	Anholt	11.52	56.72	0.026	0.065	149
DK10	Nord	-16.67	81.6	0.005	0.002	-65
DK12	Riscoe	12.09	55.69	0.040	0.120	204
ES8	Niembro	-4.85	43.44	0.069	0.064	-8
GB13	Yarner Wood	-3.71	50.6	0.064	0.076	18
GB17	Heigham Holmes	1.62	52.72	0.087	0.125	45
GB48	Auchencorth Moss	-3.24	55.79	0.020	0.049	140
IS91	Vestmannaeyjar	-20.29	63.4	0.003	0.021	526
NO2	Birkenes II	8.25	58.39	0.018	0.023	27
NO42	Zeppelin	11.89	78.91	0.059	0.005	-91
NO90	Alomar	16.01	69.28	0.003	0.015	375
SE14	Råö	11.91	57.39	0.031	0.051	62

Table B.4. *Annual sums of modelled and observed Cd wet deposition fluxes, g/km^2/year, and mean relative bias at CAMP stations in 2020.*

Code	Name	Longit	Latid	Observed	Modelled	Bias, %
BE14	Koksijde	2.66	51.12	14.7	11.8	-20
DE1	Westerland	8.31	54.93	7.5	14.0	87
DK5	Keldsnor	10.74	54.75	16.5	6.6	-60
DK8	Anholt	11.52	56.72	13.4	6.4	-52
DK12	Riscoe	12.09	55.69	18.6	9.0	-52
DK22	Sepstrup Sande	9.42	56.08	21.7	9.2	-58
DK31	Ulborg	8.43	56.29	24.5	12.0	-51
ES8	Niembro	-4.85	43.44	61.3	3.5	-94
FR90	Porspoder	-4.75	48.52	24.7	10.8	-56
GB6	Lough Navar	-7.87	54.44	0.9	2.3	165
GB13	Yarner Wood	-3.71	50.6	0.4	1.4	223
GB17	Heigham Holmes	1.62	52.72	0.3	0.8	158
GB48	Auchencorth Moss	-3.24	55.79	0.8	2.4	209
NL91	De Zilk	4.5	52.3	7.4	9.1	23
NO1	Birkenes	8.25	58.38	28.4	16.3	-43
NO39	Kårvatn	8.88	62.78	7.5	5.2	-31
SE14	Råö	11.91	57.39	27.4	12.5	-55

Table B.5. *Annual mean modelled and observed Hg air concentrations, ng/m^3, and mean relative bias at CAMP stations in 2020.*

Code	Name	Longit	Latid	Observed	Modelled	Bias, %
DK10	Nord	-16.67	81.6	1.23	1.21	-2
ES8	Niembro	-4.85	43.44	0.39	1.43	270
GB48	Auchencorth Moss	-3.24	55.79	1.64	1.30	-21
NO2	Birkenes II	8.25	58.39	1.50	1.33	-11
NO42	Zeppelin	11.89	78.91	1.44	1.23	-15
NO90	Andøya	16.01	69.28	1.42	1.26	-11
SE14	Råö	11.91	57.39	1.18	1.24	6

Table B.6. *Annual sums of modelled and observed Hg wet deposition fluxes, g/km^2/year, and mean relative bias at CAMP stations in 2020.*

Code	Name	Longit	Latit	Observed	Modelled	Bias, %
DE1	Westerland	8.31	54.93	3.14	5.66	80
ES8	Niembro	-4.85	43.44	2.93	2.38	-19
GB13	Yarner Wood	-3.71	50.6	5.00	6.16	23
GB17	Heigham Holmes	1.62	52.72	3.05	2.64	-14
GB48	Auchencorth Moss	-3.24	55.79	3.89	5.69	46
NL91	De Zilk	4.5	52.3	8.09	4.88	-40
NO1	Birkenes	8.25	58.38	7.21	9.22	28
SE14	Råö	11.91	57.39	4.18	6.75	62

The Aspect
12 Finsbury Square
London EC2A 1AS
United Kingdom

t: +44 (0)20 7430 5200
f: +44 (0)20 7242 3737
e: secretariat@ospar.org
www.ospar.org

Our vision is a clean, healthy and biologically diverse North-East Atlantic Ocean, which is productive, used sustainably and resilient to climate change and ocean acidification.

Publication Number: 973/2023

© OSPAR Commission, 2023. Permission may be granted by the publishers for the report to be wholly or partly reproduced in publications provided that the source of the extract is clearly indicated.

© Commission OSPAR, 2023. La reproduction de tout ou partie de ce rapport dans une publication peut être autorisée par l'Editeur, sous réserve que l'origine de l'extrait soit clairement mentionnée.